Pergamon

Geochimica et Cosmochimica Acta, Vol. 66, No. 21, pp. 3793–3810, 2002

0016-7037/02 $22.00 + .00

PII S0016-7037(02)00952-3

Re-Os and Pd-Ag systematics in Group IIIAB irons and in pallasites

J. H. CHEN,[1] D. A. PAPANASTASSIOU[1,2,*] and G. J. WASSERBURG[1]

[1]The Lunatic Asylum, Division of Geological and Planetary Sciences, California Institute of Technology, Mail Code 170-25, Pasadena, CA 91125, USA

[2]Earth and Space Sciences Division, Jet Propulsion Laboratory, Caltech, 4800 Oak Grove Dr., Pasadena, CA 91109-8099, USA

(*Received February* 13, 2001; *accepted in revised form May* 16, 2002)

Abstract—Using improved analytical techniques, which reduce the Re blanks by factors of 8 to 10, we report new Re-Os data on low Re and low PGE pallasites (PAL-anom) and IIIAB irons. The new pallasite samples nearly double the observed range in Re/Os for pallasites and allow the determination of an isochron of slope 0.0775 ± 0.0008 (T = 4.50 ± 0.04 Ga, using the adjusted $\lambda^{187}Re = 1.66 \times 10^{-11}$ a^{-1}) and initial $(^{187}Os/^{188}Os)_0 = 0.09599 \pm 0.00046$. If the data on different groups of pallasites (including the "anomalous" pallasites) are considered to define a whole-rock isochron, their formation would appear to be distinctly younger than for the iron meteorites by ~60 Ma. Five IIIAB irons (Acuna, Bella Roca, Chupaderos, Grant, and Bear Creek), with Re contents ranging from 0.9 to 2.8 ppb, show limited Re/Os fractionation and plot within errors on the IIAB iron meteorite isochron of slope 0.07848 ± 0.00018 (T = 4.56 ± 0.01 Ga) and initial $(^{187}Os/^{188}Os)_0 = 0.09563 \pm 0.00011$. Many of the meteorites were analyzed also for Pd-Ag and show ^{107}Ag enrichments correlated with Pd/Ag, requiring early formation and fractionation of the FeNi metal, in a narrow time interval, after injection of live ^{107}Pd ($t_{1/2}$ = 6.5 Ma) into the solar nebula. Based on Pd-Ag, the typical range in relative ages of these meteorites is ≤10 Ma. The Pd-Ag results suggest early formation and preservation of the ^{107}Pd-^{107}Ag systematics, both for IIIAB irons and for pallasites, while the younger Re-Os apparent age for pallasites suggests that the Re-Os system in pallasites was subject to re-equilibration. The low Re and low PGE pallasites show significant Re/Os fractionation (higher Re/Os) as the Re and PGE contents decrease. By contrast, the IIIAB irons show a restricted range in Re/Os, even for samples with extremely low Re and PGE contents. There is a good correlation of Re and Ir contents. The correlation of Re and Os contents for IIIAB irons shows a similar complex pattern as observed for IIAB irons (Morgan et al., 1995), and neither can be ascribed to a continuous fractional crystallization process with uniform solid-metal/liquid-metal distribution coefficients. *Copyright © 2002 Elsevier Science Ltd*

1. INTRODUCTION

High-precision, whole-rock Re-Os data have been determined on iron meteorites from Groups IAB, IIAB, IIIAB, IVA, and IVB (Shen et al., 1996; Smoliar et al., 1996a, b, 1997a, b; Chen et al., 1997; Horan et al., 1998; Birck and Allègre, 1998), using negative thermal ionization mass spectrometry (NTIMS; Heumann, 1988; Creaser et al., 1991; Völkening et al., 1991). Data on iron meteorites by two laboratories established independently a well-defined correlation line on a ^{187}Re-^{187}Os evolution diagram (Shen et al., 1996; Smoliar et al., 1996a). The data from Group IIAB give an isochron age of T = 4.61 ± 0.01 AE ($\lambda = 1.64 \times 10^{-11}$ a^{-1}) (Lindner et al., 1989) and an initial $(^{187}Os/^{188}Os)_0 = 0.09563 \pm 0.00011$ (Shen et al., 1996). To obtain nominal agreement between the age of the solar system, usually taken to be ~4.56 Ga, from U-Pb dating of silicate phases and the Re-Os whole-rock isochron age, a slightly larger decay constant for ^{187}Re can be adopted, $\lambda(^{187}Re) = 1.66 \times 10^{-11}$ a^{-1}, which is well within the uncertainty of the published value. For the rest of the paper, we will use this adjusted decay constant uniformly, and we will recalculate ages from our earlier papers, as necessary. The adjusted decay constant is dependent on the Re and Os tracer calibration in our laboratory (see "Analytical Techniques").

Previous Re-Os studies on metal phases have been restricted largely to iron meteorites, pallasites, mesosiderites, and chondrites, all with Os concentrations at the ppm-by-weight level, with corresponding Re concentrations at the 0.1-ppm level. This restriction in the samples studied was imposed largely by the Re blank, especially due to the use of CrO_3 for the oxidation of Os during sample dissolution. Limited early results on high-Ni IIIAB irons are generally consistent with the iron meteorite isochron but with much higher uncertainties (Morgan et al., 1992; Walker et al., 1993). Given the apparent tight isochronism of iron meteorites, it is important to extend the high-precision work to samples with low PGE and Re concentrations. In this work, we have adapted and developed techniques to address meteorites with lower Os concentrations (Os < 0.1 ppm). We report on high-Ni members of the IIIAB irons, with very low PGE and Re abundances. Group IIIAB is one of the largest iron meteorite groups, showing compositional trends, which suggest that the IIIAB irons were formed by extensive fractional crystallization of metallic magmas. There have been numerous attempts to model the fractional crystallization trends in IIIAB irons (e.g., Scott, 1977a, b; Jones and Drake, 1983; Haack and Scott, 1993; Ulff-Møller, 1998). However, there are problems in explaining some of the key IIIAB trends using the classic fractional crystallization models and published element partition ratios. The difficulties seem to include the proper estimation of the concentration of nonmetals (C, P, and S) in metallic magmas and the uncertainties in the solid/liquid partition ratios (D_x values). Among the 12 well-defined groups, Group IIIAB has Ir contents, which range over

* Author to whom correspondence should be addressed (dap@gps.caltech.edu).

more than three orders of magnitude, with this range being second only to that of Group IIAB. On logIr-logAu, and logIr-logAs diagrams, IIIAB irons form a broad band. Wasson (1999) has proposed a model to explain the fractionation pattern and the width of the band for IIIAB. He suggested that they resulted mainly from the trapping of parental magma within the crystallized solids. This provides an additional incentive to study low PGE, Group IIIAB irons, in which such effects may be enhanced.

For Re-Os, we have selected six samples (Acuna, Bella Roca, Chupaderos, Grant, Bear Creek, and Mt. Edith), which are members of the low-Ir (Ir $<$ 0.1 ppm) IIIB subgroup of Group IIIAB irons, to address possible time differences of formation between early and late FeNi fractional crystallization products. Based on siderophile element abundances, the metal of IIIAB irons and Main Group (MG) pallasites is considered to be consistent with fractional crystallization of metal from a common source (Davis, 1977; Scott, 1977a, b). High-precision Re-Os data were reported on metal from both MG and other distinctive pallasites (Shen et al., 1998). The pallasite Re-Os data showed a significant range in Re/Os and generally plotted within errors on the iron meteorite isochron, suggesting they crystallized within a time interval of ~20 Ma. In the study by Shen et al. (1998), some pallasites with low PGE and Re concentrations (e.g., Newport and Otinapa) had large uncertainties due to Re blanks and appeared to plot off the isochron. We have re-examined Re-Os in pallasites with low concentrations to address possible deviations from the isochron and the possibility of a larger range in Re/Os for those pallasites highly depleted in PGE and Re. We did not re-measure Newport and Otinapa due to lack of sample.

We also report Pd-Ag data on the same meteorites. In previous work, we established: (1) the presence of ^{107}Ag* (excess ^{107}Ag) in a wide variety of iron and stony-iron meteorites, (2) the in situ decay of ^{107}Pd ($t_{1/2}$ = 6.5 Ma) into ^{107}Ag in these meteorites, (3) metal-FeS internal isochrons and "whole-rock" isochrons for different metal samples of the same meteorite for a few meteorites, (4) the correlation of the "whole-rock" metal isochrons with large variations in normal Ag contents (factors of $\sim 10^3$) in the meteorites and with much smaller variations in Pd contents (factors of ~10), (5) a wide range in inferred ^{107}Pd/^{108}Pd ratios, but with many samples showing a narrow range [^{107}Pd/^{108}Pd = (1.5–2.5) $\times$ 10^{-5}], and (6) clear cases of complex behavior and disturbed systematics, relating to some sulfides and associated metal phases and attributed to shock melting (Chen and Wasserburg, 1996). The ^{107}Pd-^{107}Ag chronometer reflects the times of major chemical fractionation of Pd and Ag. This chemical fractionation is attributed to the differential condensation of Pd and Ag and to the enhanced concentration of Pd in the metal phase during planetary differentiation. If the variations in initial ^{107}Pd/^{108}Pd among meteorites indicate a time difference (ΔT) in physical-chemical segregation processes in early-formed planetesimals, then the total range in time is ΔT ~12 Ma for most meteorites. This tight cluster includes samples of IIAB, IIIAB, IVA, IVB, "anomalous" irons, and mesosiderites and pallasites. However, some meteorites exhibit no evidence of ^{107}Pd, which indicates a more recent formation, by more than ~40 Ma. With the discovery of evidence for ^{182}Hf ($t_{1/2}$ = 9 Ma) in the early solar system, it has been possible to establish another line of evidence, which points unambiguously to rapid metal or core segregation with depletion of Hf in the metal phase (Lee and Halliday, 1995; Harper and Jacobsen, 1996; Horan et al., 1998). For Re-Os in this work, we have selected from our previous studies some of these meteorites (Brenham, Glorieta Mountain, Chupaderos, Grant, Bear Creek, and Mt. Edith), which exhibit excess ^{107}Ag. We also obtained new Re-Os and Pd-Ag data in Acuna and Bella Roca.

2. ANALYTICAL TECHNIQUES

The limiting factor for studies of samples with low PGE and Re has been the procedural blank, particularly due to the use of CrO_3 for the complete oxidation of Os, which is necessary to achieve isotope exchange between sample Os and tracer Os (Shen et al., 1996; Chen et al., 1998). Aqua regia dissolution of the meteorite metal has been presented before (Shirey and Walker, 1995) and has been developed further. In this study, we have used the reverse aqua regia (RAR) technique (Chen et al., 1999; Cook et al., 2000), which permits elimination of the CrO_3 and thereby reduces the Re blanks by factors of 8 to 10.

Samples of pallasite metal were separated from silicates by a freeze-thaw process in liquid N_2. A thin layer was removed from the surfaces of the metal samples by use of a dental drill to eliminate minor rust and any remaining silicates. After cleaning in distilled ethanol, a metal sample was immediately placed in a Pyrex glass, thick-walled Carius tube. The exterior of the tube was frozen (to approximately −80°C), while the mixed Re-Os spike and a mixture of HCl : HNO_3 (1 : 3) were added. The Carius tube was sealed and then heated at 240°C for 100 h. Containment for safety was provided by a stainless steel jacket. After dissolution, OsO_4 was extracted through three stages of distillation. In the first stage, Os was distilled at 110°C from the sample solution into cold H_2O_2. Os dissolved or trapped in H_2O_2 was re-distilled into HBr. Aliquots of the HBr, containing the Os, were dried, and the Os further cleaned by microdistillation, following Roy-Barman (1993) and Birck et al. (1997). This distillation technique produces clean Os, which is ready for isotopic analysis. Re was separated by anion exchange in HNO_3 (Morgan et al., 1991; Shen et al., 1996; Chen et al., 1998). The total chemical procedure blanks for Os are $<$20 fg and are negligible. The total chemical procedure blanks for Re, which are a function of sample size and depend dominantly on the amount of acids used, range from 7.4 pg to 10.5 pg. The meteorite Re data were corrected for Re blanks, and the corrections were usually $<$1%. The filament loading blank for Os is negligible ($<$5 fg). Os was loaded on a Pt ribbon filament (0.5-mm wide $\times$ 0.03-mm thick, 99.995% pure, obtained from Electronic Space Products International [ESPI]) with a freshly prepared $Ba(OH)_2$ solution. The Re filament loading blank is 0.2 pg or less. For Re, a small amount (0.5 μL) of a suspension of fine $BaSO_4$ in water was loaded on an Ni filament (Johnson Matthey wire, 99%, 0.18-mm diameter, flattened using sapphire rods), following Birck et al. (1997). The Re sample was picked up in H_2O and loaded completely within the $BaSO_4$-covered area.

The Re and Os concentration measurements reported here and those reported by Shen et al. (1996, 1998) and Chen et al. (1998) are all based on calibrations of the Re and Os tracers using high-purity metals and not salts, which can be subject to uncertainties due to lack of stoichiometry. The uncertainty is larger in the case of Os. The data by Shen et al. (1996) and by Smoliar et al. (1996a) are in nearly complete agreement with regard to the slope of the IIAB isochron. This requires consistency in the Re/Os ratios, based on the Re and Os tracer calibrations. Repeat sets of calibrations of the Os tracer in our earlier work, using two different Os metal samples from ESPI, yielded a difference of 1.6%, indicating, most probably, some oxidation of the original Os metal samples, as received (Shen et al., 1996), and, therefore, lack of stoichiometry. A recent report (Yin et al., 2001) presents a careful calibration of the Os tracer using high-purity K_2OsCl_6, obtained from ESPI, as the gravimetric standard. These workers checked the stoichiometry of this salt by checking the gravimetry only for the K in the salt through conversion to KNO_3 and KCl. These workers also used the relatively homogeneous IIAB iron meteorite Coahuila to check for interlaboratory bias for Os concentration measurements. Their results on the sample of Coahuila that they analyzed indicate that their tracer

calibrations and ours yield results for Coahuila that are within ~1‰ of each other. This agreement is much better than the range of Os concentrations implied by our calibrations, using Os metals as gravimetric standards and better than the expected sample homogeneity. The absolute calibrations of Re and Os tracers, at the refined levels needed, require further effort.

The isotopic compositions of Re and Os were measured using NTIMS (Shen et al., 1996; Chen et al., 1998) and by using the Faraday cup collector. All Os isotope data are normalized for mass-dependent isotope fractionation by assuming the value of $^{188}Os/^{192}Os = 0.3244$ (determined as 0.324 by Nier, 1937). For reduction of the Os and Re oxide data, we use the oxygen composition $^{17}O/^{16}O = 0.00038$ and $^{18}O/^{16}O = 0.002063$, as determined from the oxides of $^{187}ReO_4^-$ (at masses 251, 252, 253, and with correction for $^{185}Re^{18}O^{16}O_3^-$; Creaser et al., 1991; Shen et al., 1996). The Pd-Ag analyses were carried out using the same techniques as described in previous reports (Chen and Wasserburg, 1983, 1990, 1996).

3. ANALYTICAL RESULTS

3.1. Re-Os Systematics

Data presentation: We define deviations (δ) in permil of the measured data (M) from a specific best-fit reference (REF) isochron as $\delta_{REF} = \{[(^{187}Re/^{188}Os)_{REF} - (^{187}Re/^{188}Os)_M]/(^{187}Re/^{188}Os)_{REF}\} \times 10^3$.

The $(^{187}Re/^{188}Os)_{REF}$ corresponds to the value of $(^{187}Re/^{188}Os)$ on the reference isochron, when $(^{187}Os/^{188}Os)_{REF} = (^{187}Os/^{188}Os)_M$. This definition attributes the deviation of a datapoint from an Re-Os isochron to the uncertainties or variations in the measured $^{187}Re/^{188}Os$. We choose this convention because for the samples under consideration, the uncertainty in $^{187}Re/^{188}Os$ dominates over the uncertainty in $^{187}Os/^{188}Os$. Furthermore, a deviation δ_{REF}, defined in terms of $(^{187}Re/^{188}Os)$, is equal to the deviation (also in permil) of the model age calculated from the datapoint from the age defined by the reference isochron. When we are discussing deviations of data from the IIAB isochron, we refer to δ_{MET} (MET = Metal), whereas when we are discussing deviations of data from the pallasite isochron, we refer to δ_{PAL}.

We have defined similar conventions in the past. For example, for Rb-Sr for extremely low Rb/Sr and non-radiogenic $^{87}Sr/^{86}Sr$ samples, we have attributed the deviations from isochrons to uncertainties in $^{87}Sr/^{86}Sr$ (Papanastassiou and Wasserburg, 1969), while for high Rb/Sr samples, for which the error propagation is analogous to the case for Re/Os data, we have attributed the deviations to $^{87}Rb/^{86}Sr$ (Albee et al., 1970). We note that Walker et al. (1993) have chosen to define deviations from an isochron by attributing them to $^{187}Os/^{188}Os$. We believe that the difference in conventions should not be confusing to the readers as long as the definitions are given explicitly.

In earlier studies, we showed that, using closed-system dissolution procedures to dissolve samples in a mixture of H_2SO_4 and CrO_3 solutions in sealed Carius tubes (SCR technique), we obtained reproducible results of good quality on iron meteorites and chondrites (Shen et al., 1996, 1998; Chen et al., 1998). The limiting factors have been the low Re concentrations and the high Re chemistry processing blank. In this study, we have used the reverse aqua regia (RAR) technique to improve Re and Os blanks. To demonstrate the reproducibility of this method, we analyzed samples of the IVA iron meteorite, Gibeon, using both the SCR and RAR techniques. The Re and Os concentrations (0.23–0.26 ppm Re and 2.4–2.7 ppm Os) in Gibeon are very high, so that the data are not sensitive to the blank correction. Using the RAR technique, we obtained Re-Os analyses of two samples of Gibeon. The results show excellent agreement in Re, Os concentrations, $^{187}Re/^{188}Os$, and $^{187}Os/^{188}Os$ ratios between two samples (Gibeon-1 and −2, Table 1) and demonstrate the excellent reproducibility of the RAR technique. For these Gibeon samples, the calculated deviations of the data from the IIAB iron best-fit line are $\delta_{MET} = 2.7 \pm 1.6$‰ and 0.0 ± 1.8‰. In comparison, two previous analyses (Gibeon-a and -b, Table 1) by Shen et al. (1996) using the SCR technique, showed ~11% lower Re and Os concentrations, comparable $^{187}Os/^{188}Os$ and $^{187}Re/^{188}Os$ ratios, and the same δ_{MET}, within uncertainties. The Re-Os results on Gibeon demonstrate the excellent reproducibility of both techniques with respect to the well-defined IIAB isochron.

3.1.1. Pallasites

All pallasite samples were analyzed using the RAR technique. The results are shown in Table 1. For the first analysis of Springwater (Springwater-1), we measured $^{187}Re/^{188}Os = 0.5185$ and $\delta_{MET} = -0.2 \pm 4.5$‰. After correcting for 7.4 pg, total Re blank, we obtain $^{187}Re/^{188}Os = 0.5177 \pm 0.001$ and $\delta_{MET} = 1.3 \pm 4.5$‰. Unless otherwise noted, the deviations δ_{MET} are given for the data corrected for Re and Os blanks. The uncertainties include the ± 2‰ uncertainty in the Re concentration due to the uncertainty in instrumental isotopic fractionation for Re. For this sample, the Re blank correction was small, and the results are the same within errors with or without blank correction. A second sample of Springwater (-2) metal yields small differences, relative to the first sample, in Re (7.98 vs. 8.31 ppb) and in Os (70.2 vs. 77.4 ppb) concentrations (Table 1), with a difference in the $^{187}Re/^{188}Os$ ratios of ~6%. There is a corresponding shift in $^{187}Os/^{188}Os$ between the two samples. In a $^{187}Os/^{188}Os$ vs. $^{187}Re/^{188}Os$ diagram (Fig. 1), both Springwater samples plot on the pallasite isochron. In the insert of Fig. 1, it can be seen that the δ_{PAL} values (5.0 ± 4.5 and 3.6 ± 4.1) plot on the isochron (the zero slope line).

The Brenham pallasite was analyzed using the same procedures. The Re and Os concentrations (2.66 ppb Re and 20.7 ppb Os) in Brenham are factors of ~3.4 lower than those in Springwater. The Brenham metal yields more radiogenic Os ($^{187}Os/^{188}Os = 0.14377 \pm 0.0001$), a higher $^{187}Re/^{188}Os$, and plots within errors on the isochron. Another pallasite, Glorieta Mountain, yields Re (1.59 ppb) and Os (10.2 ppb) concentrations, which are factors of 2 to 7 lower than in the previous two pallasites. The Re blank correction for this sample was more significant. The corrected $^{187}Re/^{188}Os$ ratio (0.7575 ± 0.0020) is 0.6% lower than the uncorrected ratios (0.7620). This sample yields the most radiogenic Os ($^{187}Os/^{188}Os = 0.15450 \pm 0.00012$) and the highest $^{187}Re/^{188}Os$ ratio among all pallasites analyzed. This sample plots within errors on the IIAB isochron, but with larger uncertainty.

The new results presented here on pallasites with low Re and Os contents extend the range of Re/Os in this group of meteorites by a factor of ~2. While it is recognized that the different pallasite groups may not be genetically related (cf. discussion in Shen et al., 1998), a best-fit line through all high-quality pallasite data (eight analyses, this work and Shen et al., 1998)

Table 1. Re-Os analytical results.

Sample	Wt. (g)	Re[1] (ng/g)	Os[1] (ng/g)	Re[2] (pg)	$^{187}Os/^{188}Os$[3]	$^{187}Re/^{188}Os$[4] (Uncorr.)	δ_{MET}[5] (Uncorr.)	$^{187}Re/^{188}Os$[6] (Corrected)	δ_{MET}[6] (Corrected)
Pallasites									
Springwater-1	0.58	8.305	77.38	7.4	0.13631 (10)	0.5185	−0.2	0.5177 (10)	1.3 (4.5)
Springwater-2	0.24	7.975	70.20	7.4	0.13862 (08)	0.5502	−4.5	0.5481 (12)	−0.6 (4.1)
Brenham	0.84	2.663	20.66	8.9	0.14377 (10)	0.6189	−9.0	0.6164 (14)	−4.9 (4.4)
Glorieta Mtn	0.98	1.590	10.15	9.5	0.15450 (12)	0.7620	−15.9	0.7575 (20)	−9.8 (4.7)
IIIB Irons									
Acuna	0.77	1.329	10.87	8.5	0.14184 (11)	0.5958	−11.8	0.5908 (17)	−3.5 (5.4)
Bella Roca	0.56	1.393	11.87	9.9	0.14059 (9)	0.5734	−1.0	0.5663 (21)	11.5 (5.7)
Bear Creek	0.82	1.200	11.44	10.5	0.13450 (20)	0.5094	−28.5	0.5040 (17)	−17.6 (8.7)
Chupaderos	0.81	1.366	10.87	8.7	0.14312 (12)	0.6111	−9.9	0.6064 (17)	−2.1 (5.4)
Grant	0.71	2.832	23.97	8.6	0.14018 (9)	0.5728	−9.0	0.5704 (13)	−4.7 (4.3)
Mt. Edith	1.00	0.8761	4.42	9.9	0.16550 (10)	0.9716	−91.4	0.9608 (33)	−79.2 (5.3)
IVA Iron									
Gibeon-1	0.27	258.5	2676		0.13226 (3)			0.46546 (35)	2.7 (1.6)
-2	0.37	258.9	2675		0.13224 (5)			0.46648 (22)	0.0 (1.8)
-a[7]	0.48	232.2	2418		0.13200 (4)			0.46290 (50)	1.1 (2.2)
-b[7]	0.33	230.9	2406		0.13202 (9)			0.46260 (40)	2.3 (3.3)

[1] Concentrations in 10^{-9} g/g.
[2] Total procedural Re blanks.
[3] Uncertainties are 2σ and are shown in parentheses.
[4,5] Uncorrected for Re blanks.
[6] Corrected for Re blanks.
[5,6] Deviations of the measured data from the IIAB reference isochron, $\delta_{MET} = \{[(^{187}Re/^{188}Os)_{REF} - (^{187}Re/^{188}Os)_M]/(^{187}Re/^{188}Os)_{REF}\} \times 10^3$, as defined in the text. For the pallasites, the deviations from the pallasite isochron (δ_{PAL}) are as follows: Springwater-1: 5.0 ± 4.5; Springwater-2: 3.6 ± 4.1; Brenham: 0.1 ± 4.4; and Glorieta Mtn: −3.3 ± 4.6.
[7] From Shen et al (1996).

yields a pallasite isochron with a slope of 0.0775 ± 0.0008 (T = 4.50 ± 0.04 Ga) and an initial $(^{187}Os/^{188}Os)_0 = 0.09599 \pm 0.00046$. In comparison, the IIAB iron meteorites yield a more precise isochron with a slope of 0.07848 ± 0.00018 (T = 4.56 ± 0.01 Ga) and an initial $(^{187}Os/^{188}Os)_0 = 0.09563 \pm 0.00011$. The data indicate that pallasites and iron meteorites crystallized within a short time interval of ~60 ± 40 Ma from sources that underwent substantial Re and Os fractionation but which had similar initial $^{187}Os/^{188}Os$ ratios.

3.1.2. IIIAB iron meteorites

We have extended the work to Group IIIAB irons with < 0.1 ppm Ir contents. The iron meteorite samples were cleaned following the same procedures as used for pallasites. Because of the low Re contents (0.88–2.83 ppb, Table 1) in these IIIAB irons, the effects of the blank corrections for Re range from 0.4 to 1.3%. In the case of the Acuna metal (Re = 1.33 ppb), the uncorrected data, $\delta_{MET} = -11.8 \pm 5.4$‰, plot slightly below the isochron, and the corrected data, $\delta_{MET} = -3.5 \pm 5.4$‰, plot within error on the isochron (Fig. 2). For Bella Roca (Re = 1.39 ppb), the uncorrected data, $\delta_{MET} = -1.0 \pm 5.7$‰, plot on the isochron, whereas the corrected data, $\delta_{MET} = 11.5 \pm 5.7$‰, plot slightly above the isochron. The deviation corresponds to only ~10 pg of Re blank correction. This shows the importance of maintaining low and reproducible Re blanks. Metal from Chupaderos also has low Re (1.37 ppb) and plots within errors on the isochron ($\delta_{MET} = -2.1 \pm 5.4$‰). A metal sample of Bear Creek yields a similar Re content (1.20 ppb), but lower $^{187}Re/^{188}Os$ and $^{187}Os/^{188}Os$ ratios. The analysis plots below the isochron ($\delta_{MET} = -17.6 \pm 8.7$). The Grant metal has a factor of ~2 higher Re (2.83 ppb) than the other IIIAB irons we analyzed. The corrected data ($\delta_{MET} = -4.7 \pm 4.3$‰) plot close to the isochron. Metal from Mt. Edith yields the lowest Re content (0.88 ppb) and high $^{187}Re/^{188}Os$ and $^{187}Os/^{188}Os$ ratios. This sample plots significantly below the isochron, corresponding to $\delta_{MET} = -79.2 \pm 5.3$. Given the uncertainties in the Re blank corrections (8.5–10.5 pg), we consider all but one of these IIIAB irons, with low PGE contents, to plot on or very close to the IIAB iron meteorite isochron (insert, Fig. 2). The new data confirm a short time interval of formation (~20 Ma) between IIIAB and IIAB irons. In contrast to other iron meteorite groups and pallasites, these IIIAB irons (with the exception of Mt. Edith) plot close to each other and show a limited range in Re/Os, despite the highly depleted Re and Os contents. The Re/Os for these IIIAB irons are distinctly higher than observed for H chondrites (Chen et al., 1998). The greatly improved blanks, as reported here, were essential for the reduction of the uncertainties in the data for these samples.

3.2. Pd-Ag Systematics

The Pd-Ag isotopic data in pallasites and IIIAB iron meteorites are shown in Table 2, which also includes the Ni and Ir data from the literature (e.g., Graham et al., 1985; Wasson, 1999). For comparison, we also list the Pd-Ag data on two pallasites (Brenham and Glorieta Mountain) and on four IIIAB irons (Chupaderos, Bear Creek, Grant, and Mt. Edith), which we reported previously (Chen and Wasserburg, 1983, 1996). New Pd-Ag data on Springwater show a high $^{108}Pd/^{109}Ag$ ratio

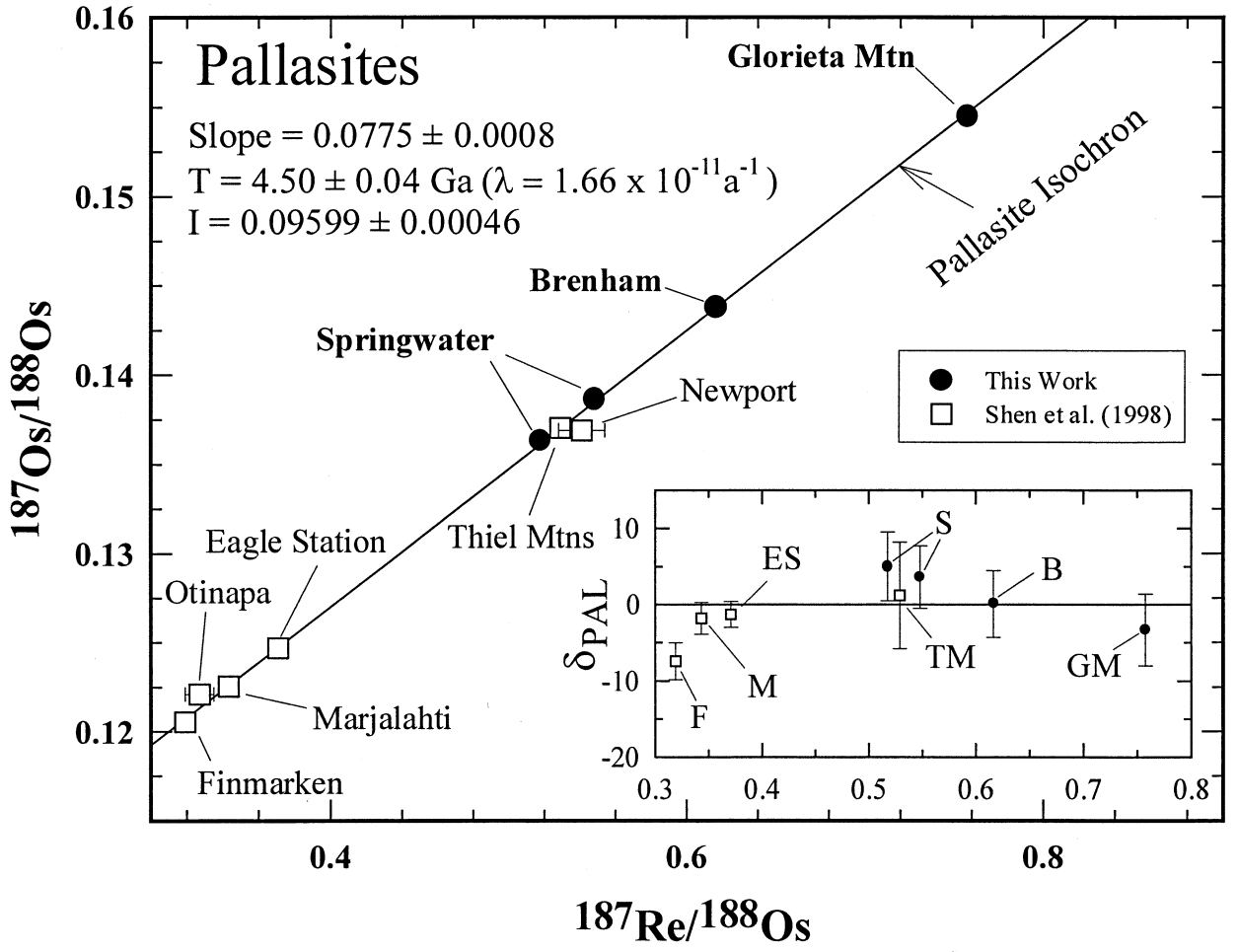

Fig. 1. ^{187}Re-^{187}Os evolution diagram for pallasites. The best-fit line shown is for pallasites, including data from this work (filled circles) and data from Shen et al (1998) (open squares). We have excluded the Otinapa and Newport data (Shen et al 1998) due to large Re blank uncertainties. The insert shows the deviations from the best-fit line (δ_{PAL}) vs. ^{187}Re/^{188}Os. All pallasite samples, except Finmarken, Otinapa and Newport, plot within errors on this isochron.

(1103 ± 2), which is a factor of ~2 higher than the two previous measurements on pallasites (Brenham and Glorieta Mountain). However, unlike the other pallasites, which show excess ^{107}Ag (Table 2, Fig. 3), the ^{107}Ag/^{109}Ag ratio in Springwater is normal, despite its higher Pd/Ag ratio. We calculate an upper limit value for $(^{107}Pd/^{108}Pd)_0 < 5.6 \times 10^{-7}$ for Springwater, which indicates that Springwater must be more than ~30 Ma younger than Gibeon. Our previous results on Eagle Station also yielded a normal Ag isotopic composition, but for a much lower measured ^{108}Pd/^{109}Ag ratio of ~190.

We obtained new Pd-Ag data on two IIIAB iron meteorites, Acuna and Bella Roca. Acuna shows a moderately high ^{108}Pd/^{109}Ag = 515 ± 1 and a clearly resolved excess δ^{107}Ag = 7.9 ± 1.8‰. In a Pd-Ag evolution diagram (Fig. 3), the Acuna data plot close to the other IIIAB irons, Bear Creek and Chupaderos, on which we reported previously. Similarly, Mt. Edith plots along this isochron, but with higher δ^{107}Ag and ^{108}Pd/^{109}Ag. The previous data on Grant metal and schreibersite show much higher ^{108}Pd/^{109}Ag ratios of 952 to 962 and yield well-resolved larger excesses, δ^{107}Ag = 14 and 19‰. In the Pd-Ag evolution diagram (Fig. 3), it appears that five high-Ni, IIIAB irons (Grant, Mt. Edith, Chupaderos, Bear Creek, and Acuna), three low-Ni IIIAB irons (Cape York, El Sampal, and Trenton), and four IIAB irons (Tocopilla, Derrick Peak, Coahuila, and Bennett County) generally plot along an isochron with a slope corresponding to $(^{107}Pd/^{108}Pd)_0$ ~2.0 × 10^{-5} and initial δ^{107}Ag = 0.0. The data for irons other than for the high-Ni IIIAB are not labeled in Fig. 3. The data on the IIAB and IIIAB irons imply that these meteorites were formed with a normal initial Ag isotopic composition and contained live ^{107}Pd with an initial $(^{107}Pd/^{108}Pd)_0$ ~2.0 × 10^{-5}. This is the same as the $(^{107}Pd/^{108}Pd)_0$ determined on Gibeon (IVA) for an internal isochron. The ^{108}Pd/^{109}Ag ratios also decrease in the following order: high-Ni IIIAB > low-Ni IIIAB > IIAB. The new data on Bella Roca plot below this isochron and yield a lower $(^{107}Pd/^{108}Pd)_0 = (1.34 \pm 0.4) \times 10^{-5}$ (Fig. 3). Two metal samples of Tres Castillos, a IIIA iron, also yield lower values for $(^{107}Pd/^{108}Pd)_0$ of (1.2 ± 0.1) × 10^{-5} and (6.5 ± 1.6) × 10^{-6}. The $(^{107}Pd/^{108}Pd)_0$ values of Bella Roca and Tres Castillos are close to the range for the pallasites, Brenham (~1.1 × 10^{-5}) and Glorieta Mountain (9.1 × 10^{-6}). Compared with the other meteorites, which plot along the Pd-Ag isochron with a

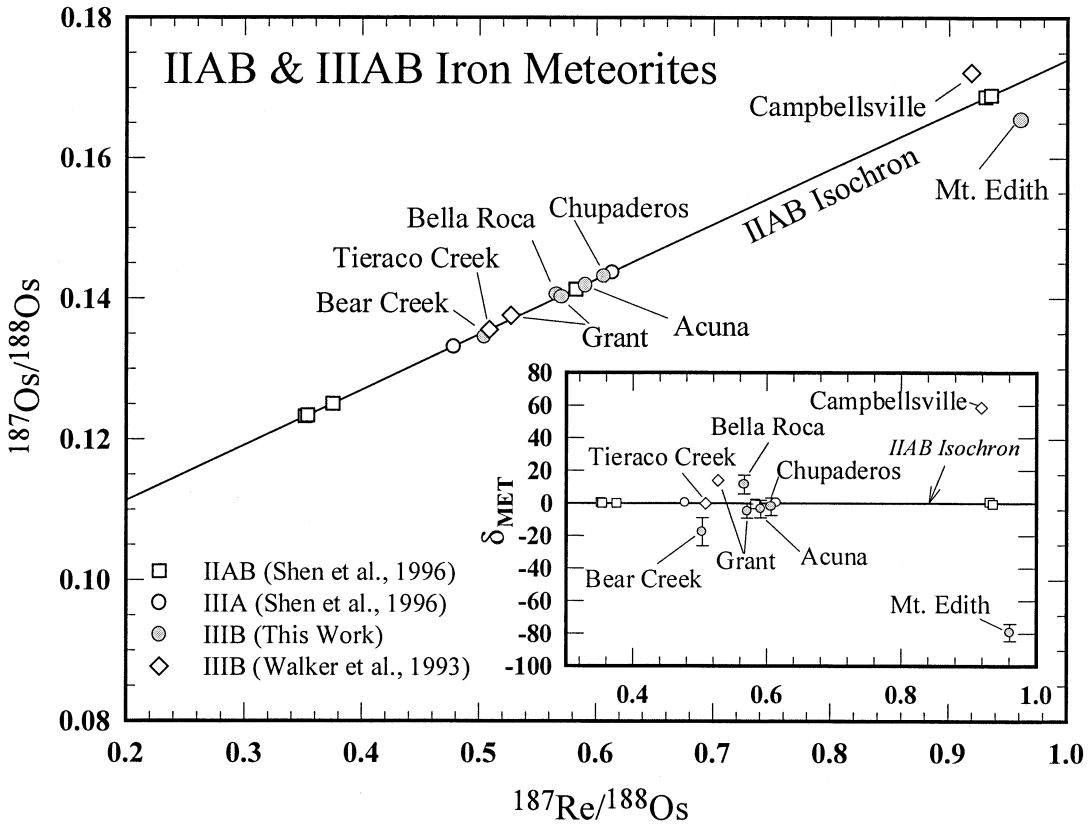

Fig. 2. ^{187}Re-^{187}Os evolution diagram for iron meteorites, including the new data on six high-Ni, low-PGE IIIAB irons. The best-fit line shown is for the IIAB irons, since that group shows a significant range in $^{187}Re/^{188}Os$. For comparison, the data from Walker et al (1993) are also shown. Most samples plot within errors on or only slightly off the IIAB isochron (Shen et al 1996). Mt. Edith and Campbellsville plot significantly away from the isochron. The insert shows the deviations δ_{MET} vs. $^{187}Re/^{188}Os$ of the data from the isochron.

slope corresponding to $(^{107}Pd/^{108}Pd)_0 \sim 2.0 \times 10^{-5}$, we calculate formation ages for these four meteorites, relative to Gibeon, which range from 4.5 Ma (Bella Roca), to 6.2 Ma (Brenham), to 8 Ma (Glorieta Mountain), and to 11 Ma (Tres Castillos). For this purpose, formation ages indicate the fractionation of Pd/Ag due to separation of the metal from silicate and sulfide phases. It follows that a large number of IIAB and IIIAB meteorites formed within ~10 Ma of each other and of most IVA and IVB irons, as argued earlier by Chen and Wasserburg (1996).

Table 2. Palladium and silver isotopic data in pallasites and IIIAB irons.[1]

Sample[2]	Ni (%)[3]	Ir (ppb)[3]	Pd (ppm)	^{109}Ag (ppb)	$^{107}Ag/^{109}Ag$	$\delta^{107}Ag$ (‰)	$^{108}Pd/^{109}Ag$
Pallasites							
Brenham	11.1	41	5.91	3.17	1.0867 ± 0.0007	5.2 ± 0.7	507 ± 1
Glorieta Mtn	12.04	14	5.72	2.88	1.0860 ± 0.0012	4.5 ± 1.1	539 ± 1
Springwater	12.6	69	7.23	1.78	1.0817 ± 0.0009	0.6 ± 0.9	1103 ± 2
IIIAB Irons							
Acuna	10.2	24	5.45	2.88	1.0896 ± 0.0019	7.9 ± 1.8	515 ± 1
Bella Roca	10.1	19	5.82	2.42	1.0898 ± 0.0025	8.1 ± 2.3	654 ± 3
Chupaderos	10	19	5.65	2.77	1.0931 ± 0.0026	11.1 ± 2.4	554 ± 3
Bear Creek	9.8	19	5.13	2.63	1.0907 ± 0.0020	8.9 ± 1.8	529 ± 4
Mt Edith	9.4	16	4.21	1.78	1.0946 ± 0.0023	12.5 ± 2.1	643 ± 5
Grant (FeNi)	9.4	42	4.9	1.40	1.1054 ± 0.0012	14.4 ± 2.0	952 ± 19
Grant (FeNiP)			5.25	1.48	1.1100 ± 0.0012	18.6 ± 2.0	962 ± 32

[1] $^{107}Ag/^{109}Ag$ ratios are all Faraday cup data. For normal Ag, $^{107}Ag/^{109}Ag = 1.0811 \pm 0.0017$.

[2] Data for Grant from Chen and Wasserburg (1983). Data for Brenham, Glorieta Mountain, Chupaderos, Bear Creek and Mt. Edith from Chen and Wasserburg (1996).

[3] Data from Wasson (1999) and Graham et al (1985).

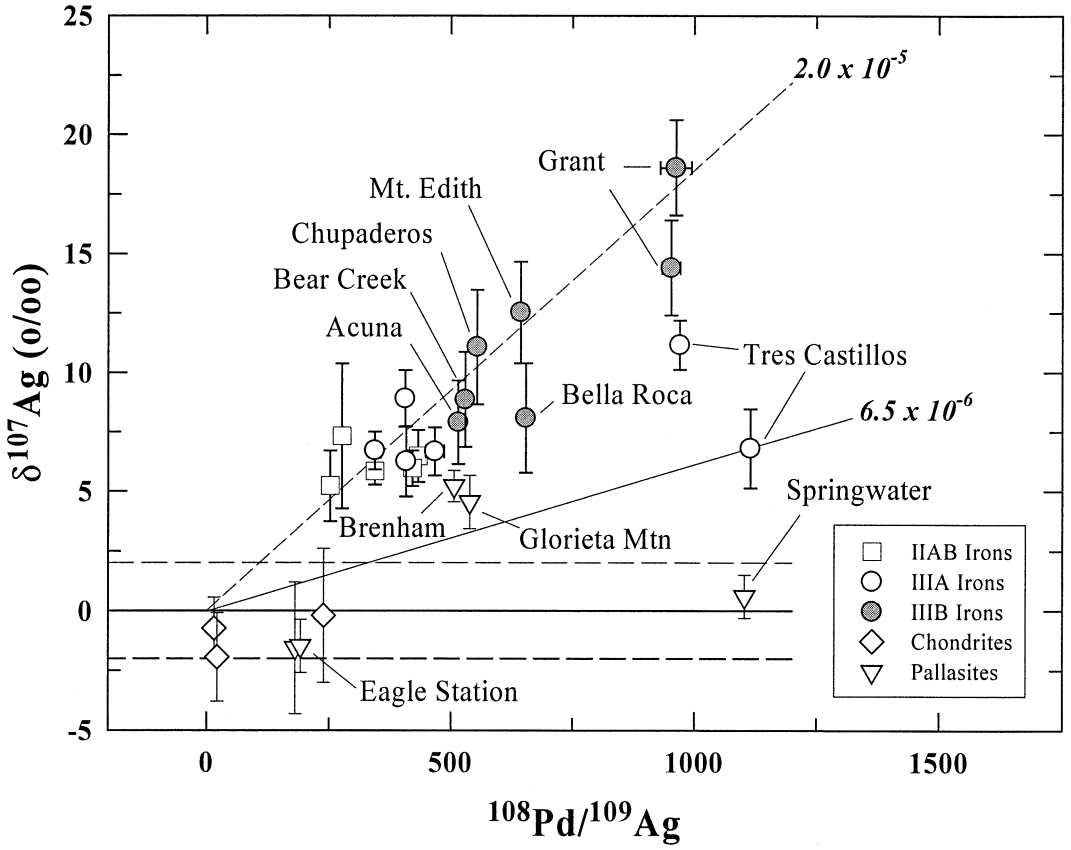

Fig. 3. ^{107}Pd-^{107}Ag evolution diagram for IIAB and IIIAB iron meteorites, pallasites, and chondrites. All iron meteorites and two pallasites show clear excesses in ^{107}Ag. Two reference isochrons, based on IIIAB irons with slopes corresponding to the initial $(^{107}Pd/^{108}Pd)_0 = 2 \times 10^{-5}$ and 6.5×10^{-6} are shown. Data for repeat analyses of Tres Castillos and Grant show different apparent initial $(^{107}Pd/^{108}Pd)_0$.

In a Pd vs. Ni diagram (Fig. 4), we show a dashed line representing the ratio of the solar abundance of Pd to Ni. Most meteorite groups generally plot along this line, but the individual meteorite groups define different and distinctive Pd/Ni trends. These suggest a fractionation pattern within each group, presumably related to fractional crystallization within each group. Most metal samples plot near the solar abundance line. By contrast, in a ^{109}Ag vs. Ni diagram (Fig. 5), there is a clear clustering of the data for individual meteorite groups. All groups of iron meteorites and pallasites plot below the solid line, which represents the solar abundance ratio. The IIIAB and IIAB irons and the pallasites plot between the two dashed lines, which correspond to depletions of Ag/Ni relative to the solar value of 10^{-2} and 10^{-3}. It is clear that the high Pd/Ag ratios in IIIAB and in pallasites are the result of Ag depletion relative to Pd. This may reflect the volatility of Ag or the removal of Ag by some other phase (Chen and Wasserburg, 1996). The identification of the Ag carrier phase and of the separation process is not yet resolved.

4. DISCUSSION

In this paper we have developed and used improved analytical techniques with low contamination levels, as required especially for Re. This has permitted us to address the Re-Os evolution of samples of those pallasites and IIIAB iron meteorites with very low Re and PGE concentrations. An important issue is the extent to which samples with very low Re and PGE contents, which presumably represent the tail end of the process of fractional crystallization for magmatic iron meteorite groups, can be argued to be coeval with those iron meteorites with high Re and PGE produced at the early stages of fractional crystallization. In addition, we had hoped that iron meteorites, which formed after extensive fractional crystallization of the parent sources, might show enhanced Re/Os fractionation and aid in a better determination of isochrons for specific "magmatic" groups of iron meteorites. This is certainly the case for pallasites, which show a wide range in Re/Os and an enhancement in Re/Os for low PGE concentrations. By contrast, the IIIAB irons that we have analyzed still continue to exhibit only a very limited range in Re/Os fractionation and do not permit the independent determination of a IIIAB Re-Os isochron. We will address the implications of the limited Re/Os fractionation in IIIAB irons and the phenomenological behavior of the Re and Os distribution coefficients. For comparison, the data by Smoliar et al. (1996a) for low-Ni IIIAB range in ^{187}Re/^{188}Os from 0.3693 (Costilla Peak) to 0.6688 (Susuman).

The distribution coefficients for Re and Os are not ade-

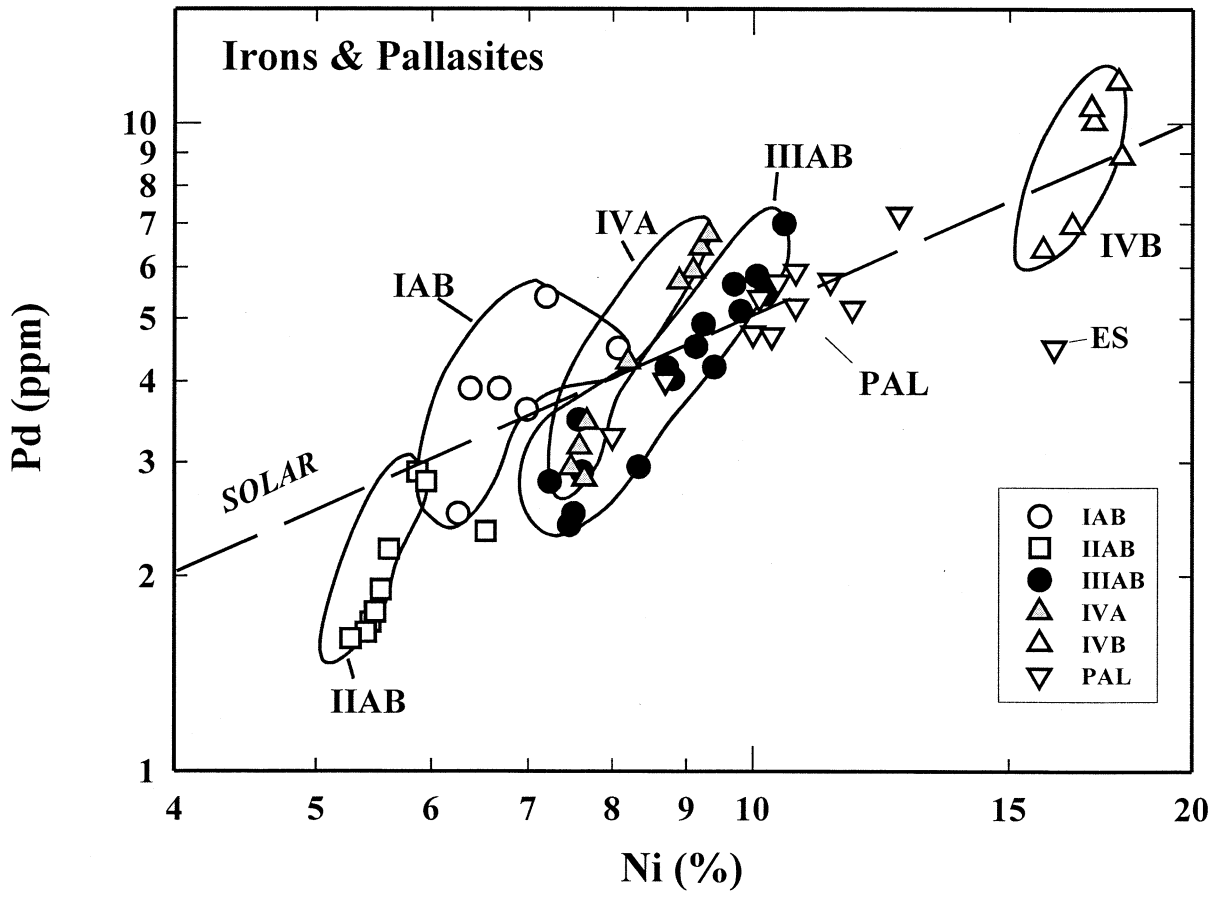

Fig. 4. LogPd vs. logNi diagram for iron meteorites, pallasites, and mesosiderites. The straight dashed line denotes the solar ratio for Pd/Ni. Most meteorite groups generally plot along this line, but within each iron meteorite group (except the nonmagmatic IAB group), the trend lines define a regular behavior of Pd/Ni, corresponding to fractional crystallization within each group. Pallasites occupy an overlapping area to the area for Group IIIAB iron meteorites, with some pallasite data extending outside the IIIAB area and along the solar Pd/Ni line. Eagle Station (ES) stands apart from any group of irons.

quately known from laboratory experiments and may be estimated only poorly from meteorite data. Walker (2000) has reviewed the status of the "siderophile element problem" in the Earth's mantle and reviewed the status of the distribution coefficients for Pt, Re, and Os, the technical and analytical problems, and the "heroic" efforts for their determination. In particular, Walker (2000) indicates (p. 2908) that Group II iron meteorites remain the best guide to the expected Re and Os fractionation patterns. Here we will compare the Re-Os and Pd-Ag evolution of pallasites and of IIIAB irons with the observations on IIAB irons.

The overall consistency of the Re-Os systematics for irons means that the events, which fractionated Re from Os, took place in a relatively narrow time interval. The actual time when this took place is dependent on the precise knowledge of the ^{187}Re decay constant. While we are using an adjusted ^{187}Re decay constant to match the age of the solar system, based on U-Pb and based on our Re and Os tracer calibrations, this does not permit the independent determination of precise, absolute Re-Os ages, since the experimental uncertainty in $\lambda(^{187}\mathrm{Re})$ of 3% (Lindner et al., 1989) corresponds to an uncertainty in age of ~135 Ma. Hence, the Re-Os data do not permit a sufficiently accurate age determination for the early solar system processes, which produced the FeNi objects. The assumed connection between the U-Pb chronometers in some stony meteorites and the crystallization ages of irons cannot be justified a priori. Fractionation in the Re-Os system is dominated by fractional crystallization processes and, hence, reflects events during early planetary evolution with metal segregation and possibly core formation. If metal melt segregations first formed and crystallized, followed later by an event of melting and recrystallization with concomitant Re-Os fractionation, then this would leave clear evidence of departures from a single isochron. If some molten FeNi cores were formed early and crystallized rapidly, while others stayed molten for, say, 100 to 200 Ma before fractional crystallization, there would be a wide scatter in the data, which is not observed for most samples. Such effects, at the level of several percent, should be readily observable. It follows that the general display of isochronous relations for Re-Os requires that metal melting, segregation, metal aggregation, core formation, and crystallization occurred over a timescale much less than 10^8 years. That early FeNi segregation events yield the original apparent isochronism requires that any later melting event did not result in Re-Os

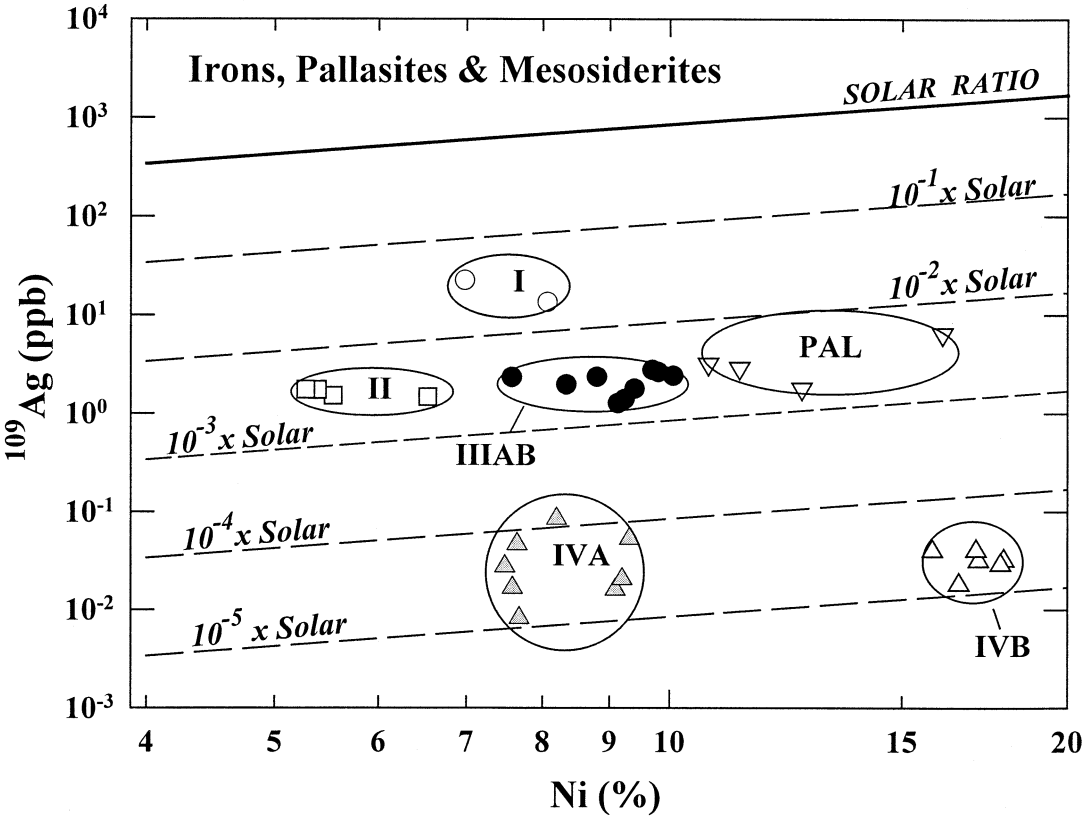

Fig. 5. Log(^{109}Ag) vs. logNi diagram for iron meteorites, pallasites, and mesosiderites. There is no correlation between Ag and Ni. All groups plot below the solid line, which represents the solar abundance ratio. The dashed lines represent different degrees of depletion of Ag relative to Ni. Groups IIAB, IIIAB, and pallasites show the same degree of Ag depletion, while Groups IVA and IVB show extreme Ag depletion, attributed to the volatility of Ag.

fractionation on a macroscopic scale from the second generation of crystallization.

Meteorite groups containing silicates, such as the pallasites, are of particular interest as they have often been considered to represent the core-mantle boundary of protoplanets. The general class of pallasites includes several subgroups. Based on similar siderophile element abundances (Scott, 1977a, b) and on the similar oxygen isotope compositions of silicates from the MG pallasites and of phosphate and chromite from IIIAB irons (Clayton and Mayeda, 1996), the MG pallasites are believed to be related to the IIIAB irons. Among the samples analyzed by Shen et al. (1998), Marjalahti, Newport, and Thiel Mountains belong to the MG pallasites, while Eagle Station shows high-Ni content and distinctive siderophile element distribution patterns and is part of the distinct Eagle Station Trio (EST). It has been noted that Finmarken has unique Ir-Ni compositions (Shen et al., 1998). The samples we analyzed in this work do not belong to the MG or the EST groups and have been termed "anomalous." For example, Brenham, with relatively high Ga and Ge contents, is identified as an anomalous (AN) member of the MG. Springwater (AN) has metal compositions appropriate to the high-Ni MG members, but its fayalite content is too high for MG trends (Scott, 1977a). Glorieta Mountain appears to be unique (Table 2) with the lowest observed Ir content (14 ppb) and high Ni (12.04%). As can be seen in Figure 1, independently of their group assignments, the pallasites are essentially consistent with a single Re-Os isochron with the possible exception of the less precise data for Otinapa and Newport (Shen et al., 1998). Therefore, the metal in pallasites from all groups and including anomalous compositions and members is consistent with differentiation at a well-defined time. This time is approximately the same as that defined by IIAB irons but possibly younger by 60 $\pm$ 40 Ma. We also note that most FeNi meteorites lie on the IIAB line. Considering the distinctive types of iron meteorites and of pallasites, there is good reason to consider them to represent different parent bodies. We recognize that the pallasites we have analyzed may well be from different protoplanets and unrelated to each other. The isochronous Re-Os relations for pallasites must reflect parallel metal melting and silicate segregation on several different planetesimals within a narrow time interval, similar to that of the IIAB iron meteorites. For FeNi, the observation of excess ^{107}Ag is associated with enrichment of Pd/Ag (primarily Ag depletion) while ^{107}Pd was still alive. In cases where the Pd-Ag systematics in sulfide have been determined to yield relatively non-radiogenic Ag, while the FeNi contains radiogenic Ag, it is apparent that the coexisting FeNi and sulfide cooled rapidly and were not remelted after the decay of ^{107}Pd (Chen and Wasserburg, 1996). By extension to the majority of cases, where internal Pd-Ag isochrons are not available, the presence of ^{107}Pd in many of these irons requires that the time of Pd-Ag fractionation be close to

the time of formation of the solar system (~4.56 Ga) and, at most, within 15 Ma. It follows that the time interval of Re-Os fractionation must also be within this narrow time interval of planetary differentiation. The dominant effect resulting in Pd-Ag fractionation is the condensation of Pd along with FeNi and the strong depletion of volatiles. We note (see above) that Brenham and Glorieta Mountains contain distinct evidence for the presence of excess ^{107}Ag. The Pd-Ag data suggest that these two pallasites formed 6 to 8 Ma later than the IIIAB Chupaderos. A possible time difference between irons and the pallasite isochron of 60 ± 40 Ma for Re-Os is not well resolved and can be viewed as being only qualitatively consistent with the Pd-Ag timescale.

With the exception of Mt. Edith, the low-PGE IIIAB irons we have analyzed display a very tight cluster in Re/Os and in ^{187}Os/^{188}Os (Fig. 2). For comparison, we have shown also the early Re-Os data on three high-Ni IIIAB irons from Walker et al. (1993). Two of their samples (Grant and Tieraco Creek) plot near the isochron and within the range of our samples. Their third sample (Campbellsville) shows high Re/Os and plots significantly above the isochron. Since the two meteorites with high Re/Os and extremely low Re (Mt. Edith and Campbellsville) yield significantly discordant Re-Os ages, we will restrict the discussion to the IIIAB analyses where Re blanks are a little less critical. The remaining analyses are concordant with a single isochron age. Most of the IIIAB data are directly consistent with the IIAB isochron. In our data, we find no evidence of parallel offsets of some samples from a single isochron, as, for example, was suggested for the Navajo group for early data, using a fusion technique, with higher Re contamination (Morgan et al., 1995). Given the small time difference between the IIAB and pallasite isochrons and the intermediate Re/Os value of the high-Ni Group IIIAB irons we analyzed, these irons are consistent also with the pallasite isochron. This would be compatible with a connection between the IIIAB irons and pallasite irons, as suggested by the siderophile element abundances for MG pallasites. However, we note again the larger range of Re/Os fractionation in pallasites compared to that in IIIAB irons. The ^{187}Re/^{188}Os range in IIIAB irons (0.37–0.67, excluding highly discordant samples) is more restricted than in pallasites (0.32–0.76) and in IIAB irons (0.39–0.94). It appears that Mt. Edith and Campbellsville should be reanalyzed.

4.1. PGE Fractionation Patterns

4.1.1. PGE fractionation and trapped melts

Under reducing conditions, only limited Re-Os fractionation during condensation processes in the early solar nebula is expected. As the PGE and Re are refractory siderophiles, when FeNi metal condensed, the siderophiles were incorporated almost exclusively into the FeNi alloys without fractionation (cf. Kelly and Larimer, 1977). Palladium, with a condensation temperature close to that of Ni, would have condensed along with the Ni, with the resulting Pd/Ni ratio being solar throughout the condensation of FeNi (Kelly and Larimer, 1977). This is reflected in Fig. 4 by the different groups of iron meteorites straddling the solar Pd/Ni line. It is also commonly assumed that only a small fraction (a few percent) of the refractory siderophiles were condensed and trapped within the Ca-Al-Ti-rich condensates in the early solar nebula. For ordinary chondrites, a small but measurable Re-Os fractionation, relative to solar abundances, was observed. In our previous report, we attributed this fractionation to reflect some transport, on a local macroscopic scale, within the chondrites, after aggregation, due to partial melting of FeNiS and redistribution of metal and sulfide. It could also represent variable Re-Os fractionation of the metal phases before the accretion of the meteorites (Chen et al., 1998). The St. Séverin chondrite is an exceptional case, with evidence for major Re-Os fractionation, which we attributed to relatively early heating of the meteorite parent body above the Fe-FeS eutectic, and to redistribution of the metal and sulfide within this chondrite.

In contrast to chondritic metal, significant fractionation of PGE, relative to Ni, is observed for the magmatic iron meteorite groups (IIAB, IIIAB, and IVA). We show in Figure 6 the correlations of Re, Os, and Ir vs. Ni. For Re and Os, we have used only the more precise isotope dilution results. We have used the Ni values from the literature rather than for the specific samples on which Re and Os were determined by isotope dilution. This may contribute to some of the scatter in the Re and Os vs. Ni plots. For the Ir vs. Ni plot, we have used literature values for both elements (Scott and Wasson, 1975; Scott 1977a, b; Graham et al., 1985; Wasson, 1999). As stressed by Scott (1972), the element patterns among groups of iron meteorites are due to nebular processes, while the trends within individual iron meteorite groups reflect fractionation processes on the parent body for each group. The PGE (Ir, Os) and Re within individual groups of iron meteorites range up to four orders of magnitude in concentrations for a small range in Ni for each iron meteorite group. These trends and correlations have been inferred to provide strong evidence for solid-metal/liquid-metal segregation and fractional crystallization on planetesimals, including core formation (Scott, 1972; Wasson, 1972; Scott and Wasson, 1975; Kelly and Larimer, 1977; Pernicka and Wasson, 1987). The more precise Re and Os data obtained by isotope dilution are, in general, supportive of this interpretation for iron meteorites. The data for the pallasites are more widely scattered. The Re and Os data on Eagle Station confirm the distinct position for this pallasite metal (and, presumably, for the other two members of the Eagle Station Trio, which have not been analyzed by isotope dilution).

A melt-trapping process has been proposed to explain the observed flattening of the Ni-Ir correlation line for IIIAB irons with high Ni and with low PGE (e.g., Ir below 90 ppb; Hassanzadeh et al., 1990) and identified clearly by Morgan et al. (1995). Wasson (1999) has also proposed a melt-trapping model to explain the wider Ir-Ni fractionation pattern for IIIAB relative to IIAB irons and the observation of relatively wide bands in Ir-Au and Ir-As diagrams for IIIAB irons. The trapping mechanism is the inclusion of coexisting parental metal magma in the crystallized FeNi solids. The PGE correlation patterns with Ni, in the MG pallasites, have also been interpreted as evidence for some trapped melt in the pallasite metal. Because sulfur is essentially insoluble in metal, Wasson (1999) has used the abundance of FeS, calculated from examination of iron meteorite slices, as a measure of the fraction of trapped liquid. Any simple fractional crystallization model produces correlated and offset tracks for the evolving parent melt and for the crystallizing instantaneous solid (Wasson, 1999). The

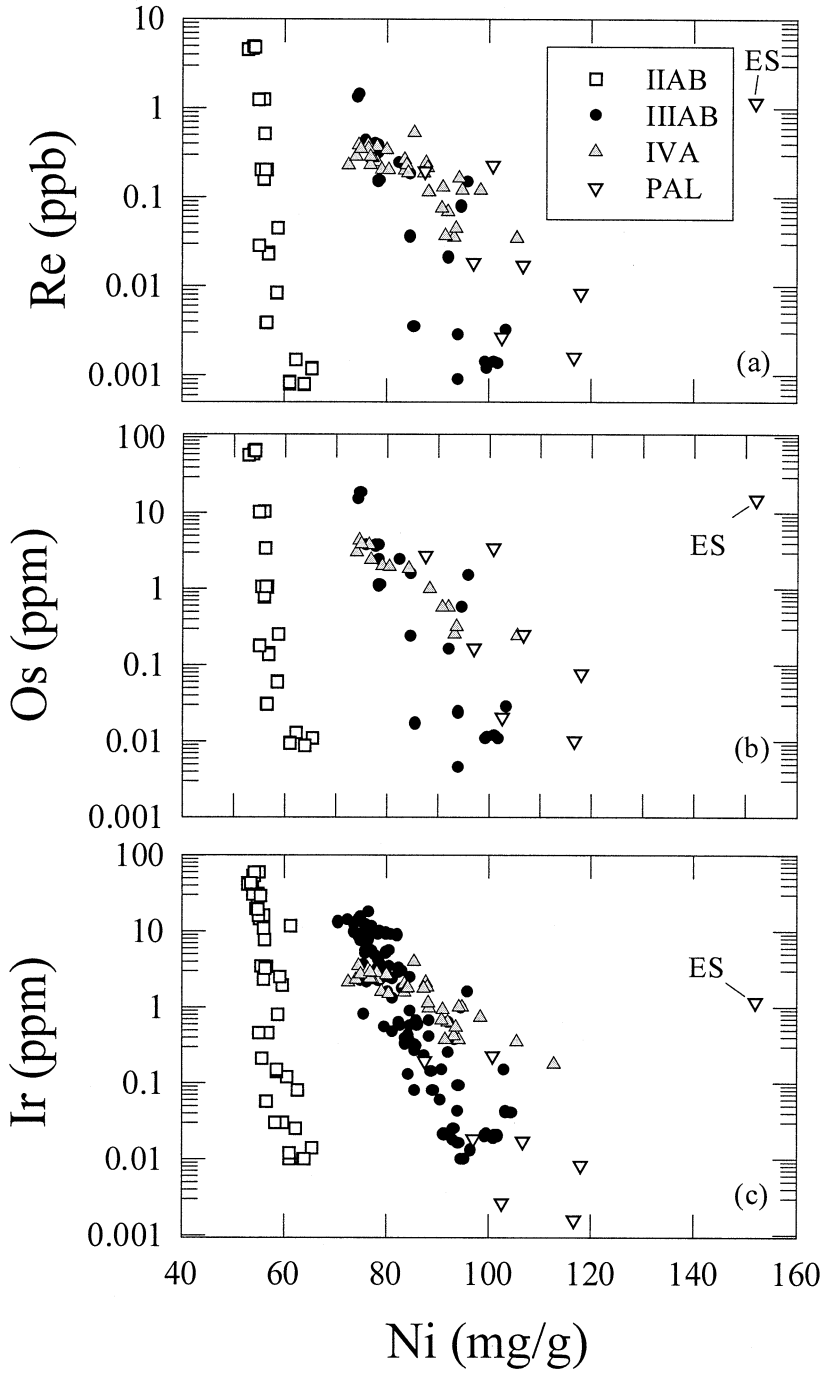

Fig. 6. Re, Os, and Ir vs. Ni diagrams for IIAB, IIIAB, IVA iron meteorites and for pallasites. See text for discussion. Eagle Station (ES) is the isolated data point in all the graphs. The large range in Re and in PGE reflects fractional crystallization. The differences in Ni contents between the groups are attributed to volatility control for the IIAB and IVA groups and to oxidation of some of the Fe by S and removal of the FeS (Kelly and Larimer, 1977) for the IIIAB.

trapped-melt model is supported by the observation that irons having higher S contents plot closer to the inferred composition of the parent liquid based on the IIIAB Ir-Au or Ir-As compositional fields. The lowest S contents are found in the irons occupying the left envelope of the IIIAB Ir-Au or Ir-As compositional fields (Wasson, 1999). We have measured several of the IIIAB irons used by Wasson (1999) for this model. Acuna, Bella Roca, Bear Creek, and Chupaderos have high S content estimates (21.7–14 mg/g; Wasson; [1999] and pers. comm., 2000, for Acuna) and plot close to each other and near the liquid tracks of the IIIAB Ir-Au or Ir-As compositional fields. The positions of these four meteorites suggest that they are mixtures of equilibrium solid and trapped melt after ~78% crystallization of the IIIAB core (Wasson, 1999). Grant has a

moderate S content (5.9 mg/g) and plots between the solid and liquid tracks in the IIIAB Ir-Au or Ir-As compositional fields (Wasson, 1999), indicating that Grant may be a mixture of equilibrium solid and trapped melt after ~75% crystallization of the IIIAB core. Based on these calculations, these IIIAB irons would be attributed to a narrow range in the fractional crystallization process. We note that in contrast to the low PGE pallasites and other iron meteorites, these high-Ni/low-PGE IIIAB iron meteorites show a very limited range in $^{187}Re/^{188}Os$ ratios (0.50–0.60). This range in $^{187}Re/^{188}Os$ falls outside the average value and range for H-chondrites ($^{187}Re/^{188}Os = 0.423 \pm 0.007$; Chen et al., 1998). The limited relative fractionation in Re/Os in these IIIAB samples is consistent with the calculation of only small relative differences in the inferred degree of fractional crystallization (75–78%). Calculations (Scott, 1977b) indicate that the compositions of metal for MG pallasites are close to the composition of the residual liquid after 80% of the IIIAB iron melt had fractionally crystallized. This can be viewed as consistent with the Re/Os in MG pallasites (Shen et al., 1998). We note that the higher Re/Os values measured in pallasites in this work are for pallasites termed "anomalous" (Springwater, Brenham, and Glorieta Mountain). Therefore, the larger range of Re/Os fractionation observed for all pallasites taken together does not present a direct conflict with the observation of a limited fractionation for IIIAB irons. This must also be considered when discussing the complexities of Re-Os fractionation (below).

4.1.2. Re-Os fractionation

While the PGE and Re show up to four orders of magnitude ranges in concentrations vs. Ni, Re/Os is only slightly fractionated as a result of these planetary differentiation processes (Pernicka and Wasson, 1987; Morgan et al., 1992). Morgan et al. (1995) presented a detailed consideration of Re and Os fractionation for the IIAB irons. These workers considered Re and Os vs. Ir correlations for IIAB irons and pointed out that Re and Ir follow a straight-line correlation on a logRe vs. logIr plot, whereas, on a logOs vs. logIr plot, the concentration data show different correlation lines for high-Ni and low-Ni IIAB irons. In Figure 7, we show the results of Morgan et al. (1995) for IIAB irons and have included our results for this group. We also show the results for the IIIAB irons from this work and from Walker et al. (1993). In the same figure, we have included the data on pallasites (Shen et al., 1998; this work) and on IVA irons (Shen et al., 1996; Smoliar et al., 1996a). In Figure 7, we have included Re and Os data by isotope dilution only, and Ir data from the literature, by neutron activation (Graham et al., 1985; Morgan et al., 1995; Wasson, 1999). In the logRe vs. logIr diagram (Fig. 7a), we confirm the observation of Morgan et al. (1995) that Re and Ir follow a straight-line relationship over nearly four orders of magnitude. The slope of the line is ~1 and corresponds to Re/Ir ~0.1. We also observe that the same correlation is essentially followed by the IIIAB data and, to first order, by the pallasite data. The Re data for pallasites appear to fall slightly above the IIAB and IIIAB straight-line correlation, especially for lower Re and Ir concentrations. The data for the IVA irons cover a more limited range in concentrations and appear to be displaced above the IIAB and IIIAB correlation line but with approximately the same slope. This strong correlation for Re and Ir suggests that both behave in a similar way under fractional crystallization of the liquid metal and with essentially equal solid-metal/liquid-metal distribution coefficients. Apparently this is the case at different absolute contents of Ni (for IIAB and IIIAB irons), independently of possible variations in S, P, C contents. It should be recognized that the Re-Ir correlation is reasonably well defined, although a log-log plot helps to de-amplify deviations from the correlation line (e.g., at the level of factors of ~2).

By comparison, in the Os-Ir plot (Fig. 7b), the high- and low-Ni endmembers of IIAB irons lie on two distinct trend lines, which indicate that processes other than simple fractional crystallization, with constant partition coefficients, are responsible for the Os-Ir fractionation. This behavior was identified by Morgan et al. (1995) who also presented extensive models for its interpretation. In this Os-Ir graph, the high-PGE/low-Ni IIIAB data plot above their counterparts in the IIAB group, while the low-PGE/high-Ni IIAB and IIIAB data overlap each other. This results in a less-pronounced break in the logOs-logIr correlation lines for the IIIAB irons relative to the IIAB irons. Similarly, the data for the pallasites and the IVA irons fall above the IIAB data. The correlations for pallasites and IVA irons are compatible with a straight-line Os-Ir correlation. We conclude that the break in the logIr-logOs correlation lines seen for the IIAB irons may be a diagnostic of specific conditions for the IIAB irons and is not as well defined for the IIIAB and IVA irons and the pallasites.

Following Morgan et al. (1995) and Shirey and Walker (1998), we plotted Os and Ir vs. Re. In Figure 8, we show the correlations for Os, Re/Os, and Re/Ir as functions of Re contents. In the logOs vs. logRe diagram (Fig. 8a), Morgan et al. (1995) noted that the low- and high-Ni IIAB irons appear to be fitted with two different straight lines (solid and dashed). This is analogous to the logOs-logIr trends and is expected, based on the straight-line correlation between logRe and logIr (Fig. 7a). Just as for logOs vs. logIr, the data on the IIIAB, the IVA, and the pallasites do not show a clear-cut break in the correlation lines as the break observed for the IIAB. In Figure 8b, we show the Re/Os ratios as a function of Re content. The trends and discontinuity for the IIAB have been identified and discussed by Morgan et al. (1995). It is difficult to explain the discontinuity in the evolution of the fractionation trends for Re/Os. The intersection of the lines is near the 0.1-ppm level for Re and may coincide with a specific composition change. In a Re/Os vs. Re diagram (Fig. 8b), there is a major change of slopes for IIAB irons at the intersection described above. For the IIAB irons, the Re/Os ratios first increase with decreasing Re contents and reach a maximum value of ~0.2; then Re/Os decrease with lower Re contents. This latter behavior is not consistent with continued fractional crystallization with constant distribution coefficients. Morgan et al. (1995) proposed that the deviation of the low-PGE/high-Ni IIB irons from a fractional crystallization line could be explained by (1) the assimilation of a small amount of primitive chondritic melt at the very end of crystallization (with $^{187}Re/^{188}Os$ ~0.4) and (2) enhanced diffusion of Os, relative to Re, from the less fractionated irons to the IIB irons with the lowest Re and Os. We observe that in this graph, the low-Ni/high-PGE IIIAB irons generally follow the IIAB irons, but the linearity of the data is not as good. For the IIIAB irons, we also observe a slower increase in Re/Os with

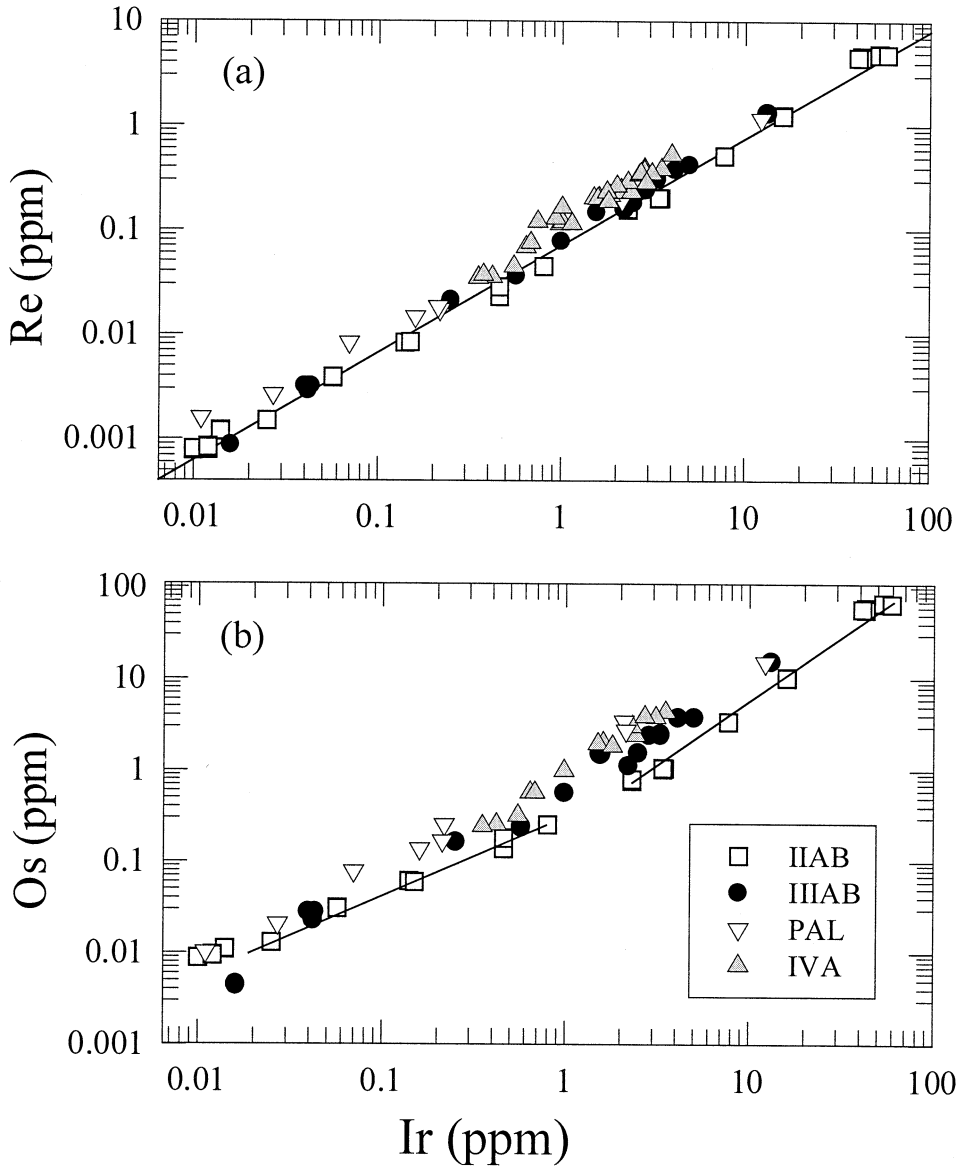

Fig. 7. (a) LogRe vs. logIr diagram for the same groups of meteorites. All meteorite groups seem to show a strong correlation between Re and Ir. The Group IVA members appear to be slightly elevated but follow the same slope as the other groups of meteorites shown. (b) LogOs vs. logIr diagram for IIAB, IIIAB, IVA iron meteorites and pallasites. The correlation lines are drawn for Group IIAB irons (from Morgan et al 1995). The IIAB irons show a general correlation of Os and Ir, but the high- and low-Ir IIAB irons fall on different slope lines. The Os-Ir data for the IIIAB, IVA, and pallasites generally plot above the correlation lines for IIAB irons. They also show a slightly larger spread and, therefore, the break in the correlation line seen for IIAB irons is less well defined for these groups of meteorites.

decreasing Re contents, relative to the IIAB irons, until a maximum Re/Os of ~0.14 at Re ~0.1 ppm is reached. With the addition of our new data on low Re and Os IIIAB endmembers (Acuna, Bear Creek, Chupaderos, and Grant, and two additional analyses of Grant and Tieraco Creek, from Walker et al., 1993), we find that the Re/Os ratios for IIIAB exhibit a nearly constant value (0.12 ± 0.01) with further decrease in Re contents (0.1–0.001 ppm). This would suggest that the relative partition coefficients for Re and Os shift to nearly equal values as fractionation proceeds and the composition of the liquid changes. Or it would suggest addition of material (such as trapped melt) with enhanced Re/Os relative to the chondritic value. We consider the observations on Re/Os fractionation for IIAB and for IIIAB to be distinct and possibly of critical importance. It is possible that the difference is due to the more oxidized nature of Group III irons relative to Group II irons (Kelly and Larimer, 1977) and possibly differences in the S or P, C abundances. However, the apparent change in Re/Os fractionation for both IIAB and IIIAB at Re and Os concentrations of ~0.1 and ~1 ppm, respectively, must indicate a well-defined process. These observations suggest the need to determine carefully Re and Os distribution coefficients as a

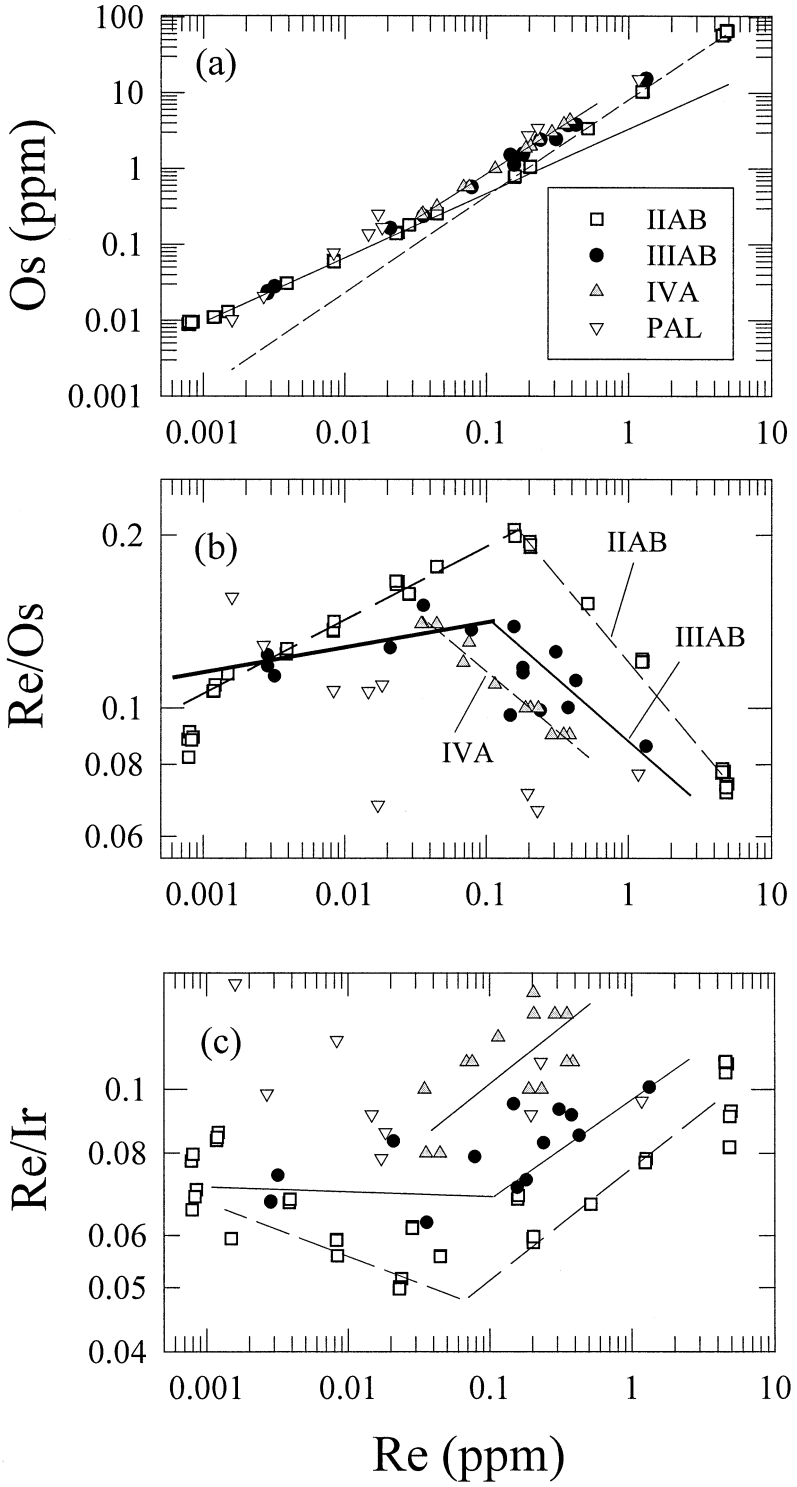

Fig. 8. (a) LogOs vs. logRe diagram in IIAB, IIIAB, IVA iron meteorites and pallasites. The lines shown are trends (with different slopes) for high- and low-Re IIAB subgroups (Morgan et al 1995). Note that in this graph, IIIAB and pallasites generally follow the trend of IIAB. However, they do not show as pronounced a change in slope as the IIAB irons. The IVA irons show a good linear array and plot parallel to and above the high-Re IIAB line. (b) Log(Re/Os) vs. logRe diagram. For IIAB, IIIAB and IVA, the lines denote similar trends for the crystallizing solids. Note the abrupt change in the slopes of IIAB and IIIAB lines at Re ~0.1 ppm: The high-Re IIIAB have a similar slope as the high-Re IIAB but show a smaller range of overall Re/Os fractionation. The low-Re IIIAB have essentially a constant Re/Os over the range of Re from ~0.1 to ~0.001 ppm. The pallasites data do not follow a well-defined trend. (c) Log(Re/Ir) vs. logRe diagram. The low-Re and high-Re IIAB and IIIAB subgroups also show changes in the slopes of the trend lines at ~0.1- to 0.01-ppm Re. Trends for IVA irons and pallasites are less well defined.

function of FeNi liquid fractional crystallization and as a function of S and P contents. We also show in Fig. 8b the data for the IVA irons. The measured samples are restricted to a narrow range in Re/Os relative to the IIIAB and IIAB irons. Even though the IVA data extend to values of Re below 0.1 ppm, they do not show a discontinuity similar to that observed for the IIAB and IIIAB samples. The IVA data follow a fractionation trend similar to those for the high-PGE/low-Ni IIAB and IIIAB irons.

In Figure 8c we show the Re/Ir measurements as a function of Re contents. We note that relative to Figure 7a, the narrow range in Re/Ir permits the use of an expanded scale for Re/Ir. This shows that there are real variations in Re/Ir by factors of ~2, which is similar to the range in Re/Os. The correlation line from Figure 7a corresponds to Re/Ir ~0.1. The Re/Ir ratios do not show strong correlations with the Re contents, as seen for Re/Os (Fig. 8b). This may be due in part to the higher precision of the Re and Os data obtained by isotope dilution.

4.1.3. Re-Os in pallasites

For pallasites, concentrations of siderophile elements in metal have defined several distinct groups: the MG, the EST, and several unique pallasites (Buseck, 1977; Davis, 1977; Scott, 1977a). Based on the oxygen isotope composition, Eagle Station silicates are similar to those in CO3 and CV3 chondrites and far removed from those in the MG pallasites and pyroxene-bearing pallasites (Clayton and Mayeda, 1996). From the oxygen isotope compositions, the silicates for the three pallasite groups require three separate parent bodies. Phosphates and chromite from IIIAB have oxygen isotope compositions consistent with those of the MG pallasites. Therefore, based on oxygen isotope composition and on siderophiles (Scott, 1977a, b), the MG pallasites are similar to IIIAB irons and distinct from the Eagle Station pallasites. However, while IIIAB irons show ~3 orders of magnitude variation in Ir contents (0.02–10 ppm) and define a good correlation with Ni, most MG pallasites have Ir contents between 0.015 and 0.2 ppm, which are not well correlated with Ni contents. Other element correlation plots also show that IIIAB irons and MG pallasites occupy adjacent but non-overlapping regions, indicating that the connection between these two groups of meteorites is limited. In Fig. 8b, the Re-Os data on pallasites do not show an identifiable pattern or a pattern similar to any of those for the other iron groups presented.

Based on REE data, Davis and Olsen (1991, 1996) suggested that the olivine in pallasites may not necessarily reflect simple planetary differentiates. During the process of pallasite formation by mixing silicates and metal, it was possible to incorporate extraneous components, including materials with highly fractionated REE patterns. Mathew and Begemann (1997) reported solar-like trapped noble gases in the Brenham pallasite. The trapping of solar gases in a minor phase and the low-energy proton irradiation must have occurred on the regolith of the Brenham parent body before assembly of the metal and silicate. Therefore, we would consider some of the pallasites not as representatives of core-mantle boundaries, but as more complex breccias, with at least a stage of formation or assembly on the surfaces of parent planets. While the siderophile elements and the REE and oxygen isotopes suggest diverse sources for the components of the pallasites, the well-defined Re-Os isochron for pallasites requires that the FeNi in pallasites from different sources still reflect essentially isochronous Re-Os fractionation processes that occurred very early in the solar system. Given the evidence for distinct pallasite groups, the pallasite isochron must be considered as a total rock isochron of independent differentiates, each sharing the attribute of early and essentially isochronous formation.

4.2. Short-Lived Parent-Daughter Systems

Mn-Cr data on MG pallasites as well as on Eagle Station, indicate the presence and in situ decay of live ^{53}Mn (half-life 3.7 Ma) (Birck and Allègre, 1988; Lugmair and Shukolyukov, 1998). A comparison of ^{107}Pd and ^{53}Mn chronometers on the same meteorites is possible for a few samples (cf. Chen and Wasserburg; [1996] and earlier discussion). In the case of Cape York, ^{107}Pd/^{108}Pd and ^{53}Mn/^{55}Mn show initial values of 2.5×10^{-5} and 2.2×10^{-5}, respectively. In other cases, Group IIIAB irons (e.g., Grant, Bear Creek, Mt. Edith, and Chupaderos) show ^{107}Pd/^{108}Pd $\sim 2 \times 10^{-5}$, but much smaller ^{53}Mn/^{55}Mn (1×10^{-6} to 2.4×10^{-5}). In addition, ^{107}Pd is absent in the metal of Eagle Station, but the olivine and chromite yield ^{53}Mn/^{55}Mn $= 2.3 \times 10^{-6}$. Phosphate and olivine in Springwater show excess ^{53}Mn with ^{53}Mn/^{55}Mn $= (1.4 \pm 0.4) \times 10^{-5}$, but ^{107}Pd is absent in the metal of Springwater. There appear to be major discrepancies between the ^{107}Pd and ^{53}Mn chronometers. We conclude that a more intensive comparative study of the ^{107}Pd-^{107}Ag and ^{53}Mn-^{53}Cr systems is necessary, which may aid a detailed comparison with the Re-Os isotope systems.

Extensive W isotope data on iron meteorites show relatively uniform depletions of ^{182}W, reflecting early Hf-W fractionation, before the decay of ^{182}Hf ($t_{1/2}$ = 9 Ma) (Lee and Halliday 1995, 1996; Harper and Jacobsen, 1996; Jacobsen and Harper, 1996; Horan et al., 1998). The ^{182}W depletions in iron meteorites reflect the separation of silicates and metal. Based on the ^{182}W isotope data, that process was of short duration, $<$ ~5 Ma. However, once W is isolated from Hf, the isotope composition of W becomes an invariant and does not provide a measure of the passage of time unless the metal becomes re-equilibrated with silicates. By contrast, Re and Os fractionation in iron meteorites depends on fractional crystallization from liquid metal and is not related to metal-silicate segregation. The Re-Os fractionation from FeNi melt crystallization occurred over a short timescale ($<$ 40 Ma) but occurred after the Hf-W fractionation that accompanied metal-silicate segregation. In the absence of metal-silicate re-equilibration, subsequent to the original metal-silicate segregation, the timescale defined by the Re-Os and Pd-Ag systems would not be reflected in the W isotope systematics of iron meteorites. At present, there are a few Pd-Ag internal isochrons but no ^{182}Hf-^{182}W internal isochrons on iron meteorites. For low metamorphic grade chondrites, Lee and Halliday (2000) have reported on the Hf-W systematics for magnetic (metal) and non-magnetic (silicates and some metal) separates. The data show depletions in ^{182}W/^{184}W in the chondritic metal, similar to those found for iron meteorites. For the non-magnetic separates, the ^{182}W/^{184}W is close to normal. These data have been interpreted as defining internal isochrons (Lee and Halliday, 2000). The Hf-W data on

the non-magnetic, silicate-rich separates do not appear to directly reflect and represent complementary material, enriched in Hf/W, and from which W had been removed, to become resident in the metal in the chondrites. Therefore, the data can also be consistent with the chondrites being a mixture of early fractionated metal and of silicates, the latter of which did not become depleted in W and enriched in Hf/W. In such a case, the existing Hf-W data on chondrites would define the timescale of Hf-W fractionation in the environment that produced the metal grains. The admixed silicate material could represent matter that had not fractionated Hf from W. The timescale defined for the Hf/W fractionation for chondritic metal in the nebula is essentially the same as that defined by consideration of iron meteorites and the data on the bulk carbonaceous meteorites Allende and Murchison (Lee and Halliday, 1995). In general, it is clear from both the ^{107}Pd-^{107}Ag and ^{182}Hf-^{182}W systems that metal segregation and planetary core formation started on various planetesimals within a few million years. The processes that occurred for Pd-Ag require major Ag depletion in the metal, and for Hf-W they require silicate-metal segregation. The Pd-Ag fractionation has been explained by early condensation processes in a hot region of the solar nebula (Kelly and Larimer, 1977; Kelly and Wasserburg, 1978; Chen and Wasserburg, 1996). There are no major Pd-Ag fractionation mechanisms that can obviously be related to Fe-S, Fe-Ni, and silicate segregation in planetesimals. The conditions for a hot nebula with physical segregation of FeNi are not readily understandable from current models. There are clear gaps in our understanding of key processes in the early solar system. However, the short timescale for formation and segregation of FeNi metal is essentially fixed.

From the Pd-Ag systematics in iron meteorites with internal isochrons (sulfide-metal), it is evident that, after melting, the FeNi solidified sufficiently rapidly to preserve the isotopic differences between FeS and FeNi. If this melting took place along with silicate-metal equilibration, then this would also generate the observed ^{182}W effects. If the timescales for crystallization of the liquid metal (into metal and sulfide) and for cooling were short compared to 10 Ma, then this would yield Pd-Ag internal isochrons with ^{107}Pd/^{108}Pd $\sim 2 \times 10^{-5}$ and give the observed deficits in ^{182}W in the metal. If the timescales were longer, and if sulfides were then separated late on a macroscopic or large scale from the Fe-Ni melt, then there would be some radiogenic ^{107}Ag* in the sulfide (depending on the Pd/Ag of the bulk) and still excesses in ^{107}Ag and deficits in ^{182}W in the metal, as observed. For a more extensive discussion of the Pd-Ag system, including the possibility of moderate enrichment of Pd/Ag in FeNi due to FeS-FeNi separation on planetary bodies, see Chen and Wasserburg (1996).

The Re-Os system reflects the metal crystallization process, but the absolute time is not fixed on a timescale of $\sim$100 Ma due to the uncertainty in the half-life of ^{187}Re. The Re-Os data are compatible, for most samples, with the short timescale for melting and crystallization given by ^{107}Pd-^{107}Ag. It is expected that FeNi cores would have persisted in a molten state for timescales of over a few 10^7 years in planetesimals over $\sim$50 km in radius. We, therefore, infer that the Re-Os whole-rock isochron most likely represents the result of melting and crystallization of planetesimals that were smaller than $\sim$100 km in radius. Some larger bodies persisted with molten metal cores, including those that were presumably responsible for mesosiderites. These objects should show distinctive behavior for the Pd-Ag, Hf-W, and Re-Os systems.

5. CONCLUSIONS

This work has led to the following conclusions:

1. New, low Re-blank techniques permit the reliable analysis of very low Re and PGE iron meteorites.
2. Re-Os data on IIIAB irons show a relatively limited range in Re/Os, which does not permit the calculation of a precise isochron However, the Re-Os systematics of the IIIAB irons are consistent with the isochron for IIAB irons and with early and rapid formation.
3. Re-Os data on low Re and PGE pallasites extend the range in Re/Os and permit the determination of a precise whole-rock isochron, corresponding to an age that is younger by $\sim$60 Ma than for the iron meteorite whole-rock isochron The pallasite isochron is defined by members of the MG of pallasites, by Eagle Station, and by anomalous pallasites. With respect to an isochronous formation, the Re-Os data on pallasites do not distinguish between different pallasite groups.
4. Correlations of Re and Ir are consistent, within the precision of the data, with a model of continuous fractionation by melting and fractional crystallization Correlations of Re and Os show more complex patterns, which are not consistent with a constancy of the solid/liquid distribution coefficients during the fractional crystallization.
5. IIIAB and IIAB irons follow similar complex behavior as fractional crystallization proceeds This behavior is not as clearly seen for pallasites.
6. Pd-Ag analyses on the same samples analyzed for Re-Os show distinct evidence for excess ^{107}Ag and for the initial presence of live ^{107}Pd This is consistent with an early timescale of formation and with the Re-Os timescale. Agreement of the ^{107}Pd-^{107}Ag chronology with other short-lived nuclide chronologies, such as for ^{53}Mn-^{53}Cr, is still elusive.

Acknowledgments—This paper is dedicated to Dick Holland, who has been known to one of the authors, since his early radiation damage days, and to the other authors, since he began exhaling atmospheres and bringing forth oceans. We thank Richard J. Walker and Uli Ott for substantive and detailed reviews and attention to the paper. This work was supported by NASA Grant NAG5-8251. This is GPS Division Contribution No. 8730(1061).

Associate editor: U. Ott

REFERENCES

Albee A. L., Burnett D. S., Chodos A. A., Haines E. L., Huneke J. C., Papanastassiou D. A., Podosek F. A., Russ G. P., III, and Wasserburg G. J. (1970) Mineralogic and isotopic investigations on lunar rock 12013. *Earth Planet. Sci. Lett.* **9,** 137–163.

Birck J. L. and Allègre C. J. (1988) Manganese-chromium isotope systematics and the development of the early solar system. *Nature.* **331,** 579–584.

Birck J. L. and Allègre C. J. (1998) Rhenium-187–osmium-187 in iron meteorites and the strange origin of the Kodaikanal meteorite. *Meteorit. Planet. Sci.* **33,** 647–653.

Birck J. L., Roy-Barman M., and Capmas F. (1997) Re-Os isotopic measurements at the femtomole level in natural samples. *Geostand. Newsl.* **21,** 19–27.

Buseck P. R. (1977) Pallasite meteorites–mineralogy, petrology, and geochemistry. *Geochim. Cosmochim. Acta.* **41,** 711–740.

Chen J. H. and Wasserburg G. J. (1983) The isotopic composition of silver and lead in two iron meteorites: Cape York and Grant. *Geochim. Cosmochim. Acta.* **47,** 1725–1737.

Chen J. H. and Wasserburg G. J. (1990) The isotopic composition of Ag in meteorites and the presence of ^{107}Pd in protoplanets. *Geochim. Cosmochim. Acta.* **54,** 1729–1743.

Chen J. H. and Wasserburg G. J. (1996) Extinct ^{107}Pd in the early solar system and implications for planetary evolution. In *Earth Processes: Reading the Isotopic Code* (eds. A. Basu and S. Hart). *Geophysical Monograph 95,* AGU, 1–20.

Chen J. H., Papanastassiou D. A., and Wasserburg G. J. (1997) Re-Os systematics in chondrites and iron meteorites. *Lunar Planet. Sci. XXVIII*. Lunar Planet. Inst., Houston, 221–222(abstract).

Chen J. H., Papanastassiou D. A., and Wasserburg G. J. (1998) Re-Os systematic in chondrites and the fractionation of the platinum group elements in the early solar system. *Geochim. Cosmochim. Acta.* **62,** 3379–3392.

Chen J. H., Papanastassiou D. A., and Wasserburg G. J. (1999) Re-Os systematics in the Allende CAI: Big Al. *Lunar Planet. Sci. XXX*. Lunar Planet. Inst., Houston, #1483 (abstract).

Clayton R. N. and Mayeda T. K. (1996) Oxygen isotope studies of achondrites. *Geochim. Cosmochim. Acta.* **60,** 1999–2017.

Cook D. L., Walker R. J., and Horan M. F. (2000) New applications of the ^{187}Re-^{187}Os and ^{190}Pt-^{186}Os isotope systems to the study of iron meteorites. *Lunar Planet. Sci. XXXI*. Lunar Planet. Inst., Houston, #1347 (abstract).

Creaser R. A., Papanastassiou D. A., and Wasserburg G. J. (1991) Negative thermal ion mass spectrometry of osmium, rhenium, and iridium. *Geochim. Cosmochim. Acta.* **55,** 397–401.

Davis A. M. (1977) *The cosmochemical history of pallasites*. Ph.D. thesis, Yale University.

Davis A. M. and Olsen E. J. (1991) Phosphates in pallasite meteorites as probes of mantle processes in small planetary bodies. *Nature.* **353,** 637–640.

Davis A. M. and Olsen E. J. (1996) REE patterns in pallasite phosphates–a window on mantle differentiation in parent bodies. *Meteorit. Planet. Sci.* **31,** A34–A35 (abstract).

Graham A. L., Bevan A. W. R., and Hutchison R. (1985) *Catalogue of Meteorites*. Univ. of Arizona Press, Tucson.

Haack H. and Scott E. R. D. (1993) Chemical fractionations in group IIIAB iron meteorites: Origin by dendritic crystallization of an asteroidal core. *Geochim. Cosmochim. Acta.* **57,** 3457–3472.

Harper C. L. and Jacobsen S. B. (1996) Evidence for ^{182}Hf in the early solar system and constraints on the timescale of terrestrial accretion and core formation. *Geochim. Cosmochim. Acta.* **60,** 1131–1153.

Hassanzadeh J., Rubin A. E., and Wasson J. T. (1990) Compositions of large metal nodules in mesosiderites: Links to iron meteorite group IIIAB and the origin of mesosiderite subgroups. *Geochim. Cosmochim. Acta.* **54,** 3197–3208.

Heumann K. G. (1988) Isotope dilution mass spectrometry. In *Inorganic Mass Spectrometry*. (eds. F. Adams et al.), chap. 7 John Wiley & Sons, New York, pp. 301–376 .

Horan M. F., Smoliar M. I., and Walker R. J. (1998) ^{182}W and ^{187}Re-^{187}Os systematics of iron meteorites: Chronology for melting, differentiation, and crystallization in asteroids. *Geochim. Cosmochim. Acta* **62,** 545–554.

Jacobsen S. B. and Harper C. L., Jr. (1996) Accretion and early differentiation history of the earth based on extinct radionuclides. In *Earth Processes: Reading the Isotopic Code* (eds. A. Basu and S. Hart), *Geophysical Monograph 95*, AGU, pp. 47–74, *Geophysical Monograph 95,* AGU.

Jones J. H. and Drake M. J. (1983) Experimental investigations of trace element fractionation in iron meteorites, II: The influence of sulfur. *Geochim. Cosmochim. Acta.* **47,** 1199–1209.

Kelly W. R. and Larimer J. W. (1977) Chemical fractionations in meteorites-VIII. Iron meteorites and the cosmochemical history of the metal phase. *Geochim. Cosmochim. Acta.* **41,** 93–111.

Kelly W. R. and Wasserburg G. J. (1978) Evidence for the existence of ^{107}Pd in the early solar system. *Geophys. Res. Lett.* **5,** 1079–1082.

Lee D.-C. and Halliday A. N. (1995) Hafnium-tungsten chronometry and the timing of terrestrial core formation. *Nature*. **378,** 771–774.

Lee D.-C. and Halliday A. N. (1996) Hf-W isotopic evidence for rapid accretion and differentiation in the early solar system. *Science.* **274,** 1876–1879.

Lee D.-C. and Halliday A. N. (2000) Hf-W isotopic systematics of ordinary chondrites and the initial ^{182}Hf/^{180}. Hf of the solar system.. *Chem. Geol.* **169,** 35–43.

Lindner M., Leich D. A., Russ G. P., Bazan J. M., and Borg R. J. (1989) Direct determination of the half-life of ^{187}Re. *Geochim. Cosmochim. Acta.* **53,** 1597–1606.

Lugmair G. W. and Shukolyukov A. (1998) Early solar system timescales according to ^{53}Mn-^{53}Cr systematics. *Geochim. Cosmochim. Acta.* **62,** 2863–2886.

Mathew K. J. and Begemann F. (1997) Solar-like trapped noble gases in the Brenham pallasite. *J. Geophys. Res.* **102,** 11015–11026.

Morgan J. W., Golightly D. W., and Dorrzapf A. F. (1991) Methods for the separation of rhenium, osmium and molybdenum to isotope geochemistry. *Talanta.* **38,** 259–265.

Morgan J. W., Walker R. J., and Grossman J. N. (1992) Rhenium-osmium isotope systematics in meteorites I: Magmatic iron meteorite groups IIAB and IIIAB. *Earth Planet. Sci. Lett.* **108,** 191–202.

Morgan J. W., Horan M. F., Walker R. J., and Grossman J. N. (1995) Rhenium-osmium concentration and isotope systematics in group IIAB iron meteorites. *Geochim. Cosmochim. Acta.* **59,** 2331–2344.

Nier A. O. (1937) The isotopic constitution of osmium. *Phys. Rev.* **52,** 885.

Papanastassiou D. A. and Wasserburg G. J. (1969) Initial strontium isotopic abundances and the resolution of small time differences in the formation of planetary objects. *Earth Planet. Sci. Lett.* **5,** 361–376.

Pernicka E. and Wasson J. T. (1987) Ru, Re, Os, Pt, and Au in iron meteorites. *Geochim. Cosmochim. Acta.* **51,** 1717–1726.

Roy-Barman M. (1993) Mesure du rapport ^{187}Os/^{186}Os dans les basaltes et les péridotites: Contribution à la systématique ^{187}Re-^{187}Os dans le manteau. Ph.D. thesis, University of Paris 7.

Scott E. R. D. (1972) Chemical fractionation in iron meteorites and its interpretation. *Geochim. Cosmochim. Acta.* **36,** 1205–1236.

Scott E. R. D. (1977a) Pallasite-metal composition, classification and relationships with iron meteorites. *Geochim. Cosmochim. Acta* **41,** 349–360.

Scott E. R. D. (1977b) Geochemical relationships between some pallasites and iron meteorites. *Mineral. Mag.* **41,** 265–272.

Scott E. R. D. and Wasson J. T. (1975) Classification and properties of iron meteorites. *Rev. Geophys. Space Phys.* **13,** 527–546.

Shen J. J., Papanastassiou D. A., and Wasserburg G. J. (1996) Precise Re-Os determinations and systematics of iron meteorites. *Geochim. Cosmochim. Acta.* **60,** 2887–2900.

Shen J. J., Papanastassiou D. A., and Wasserburg G. J. (1998) Re-Os systematics in pallasite and mesosiderite metal. *Geochim. Cosmochim. Acta.* **62,** 2715–2723.

Shirey S. B. and Walker R. J. (1995) Carius tube digestion for low blank Re-Os analysis. *Anal. Chem.* **67,** 2136–2141.

Shirey S. B. and Walker R. J. (1998) Re-Os isotopes in cosmochemistry and high temperature geochemistry. *Ann. Rev. Earth Planet. Sci.* **26,** 423–500.

Smoliar M. I., Walker R. J., and Morgan J. W. (1996a) Re-Os ages of group IIA, IIIA, IVA, and IVB iron meteorites. *Science.* **271,** 1099–1102.

Smoliar M. I., Walker R. J., and Morgan J. W. (1996b) Re-Os isotope systematics in the Cape York meteorite shower. *Lunar Planet. Sci. XXVII*. Lunar Planet. Inst., Houston, 1225–1226 (abstract).

Smoliar M. I., Walker R. J., and Morgan J. W. (1997a) Re-Os isotopic constraints on the crystallization history of IIAB iron meteorites. *Lunar Planet. Sci. XXVIII*. Lunar Planet. Inst., Houston, 1341–1342 (abstract).

Smoliar M. I., Walker R. J., and Morgan J. W. (1997b) Re-Os isochron for IA meteorites–further refinement of the Rhenium-187 decay constant. *Meteorit. Planet. Sci.* **32,** A122–A123 (abstract).

Ulff-Møller F. (1998) Effects of liquid immiscibility on trace element fractionation in magmatic iron meteorites: A case study of Group IIIAB. *Meteorit. Planet. Sci.* **33,** 207–220.

Völkening J., Walczyk T., and Heumann K. G. (1991) Osmium isotope ratio determinations by negative thermal ionization mass spectrometry. *Int. J. Mass Spectrom. Ion Proc.* **105,** 147–159.

Walker D. (2000) Core participation in mantle geochemistry. *Geochim. Cosmochim. Acta.* **64,** 2897–2911.

Walker R. J., Morgan J. W., Horan M. F., and Grossman J. N. (1993) Rhenium-Osmium isotope systematics of ordinary chondrites and iron meteorites. *Lunar Planet. Sci. XXIV*. Lunar Planet. Inst., Houston, 1477–1478 (abstract).

Wasson J. T. (1972) Parent-body models for the formation of iron meteorites. *Proc. Intl. Geol. Cong.* **24,** 161–168.

Wasson J. T. (1999) Trapped melt in IIIAB irons; solid/liquid elemental partitioning during the fractionation of the IIIAB magma. *Geochim. Cosmochim. Acta.* **63,** 2875–2889.

Yin Q. Z., Jacobsen S. B., Lee C.-T., McDonough W. F., Rudnick R. L., and Horn I. (2001) A gravimetric K_2OsCl_6 standard: Application to precise and accurate Os spike calibration. *Geochim. Cosmochim. Acta* **65,** 2113–2127.